Annu. Rev. Mar. Sci. 2016. 8:X–X
doi: 10.1146/annurev-marine-052915-100829

<doi>10.1146/annurev-marine-052915-100829</doi>

Changes in Ocean Heat, Carbon Content, and Ventilation: A Review of the First Decade of GO-SHIP Global Repeat Hydrography

L.D. Talley,[1] R.A. Feely,[2] B.M. Sloyan[3], R. Wanninkhof,[4] M.O. Baringer,[4] J.L. Bullister,[2] C.A. Carlson,[5] S.C. Doney,[6] R.A. Fine,[7] E. Firing,[8] N. Gruber,[9] D.A. Hansell,[7] M. Ishii,[10] G.C. Johnson,[2] K. Katsumata,[11] R.M. Key,[12] M. Kramp,[13] C. Langdon,[7] A.M. Macdonald,[6] J.T. Mathis,[2] E.L. McDonagh,[14] S. Mecking,[15] F.J. Millero,[7] C.W. Mordy,[2,16] T. Nakano,[17] C.L. Sabine,[2] W.M. Smethie,[18] J.H. Swift,[1] T. Tanhua,[19] A.M. Thurnherr,[18] M.J. Warner,[20] and J.-Z. Zhang[4]

*Author affiliations can be found in the Acknowledgments section.

Keywords anthropogenic climate change, ocean temperature change, salinity change, ocean carbon cycle, ocean oxygen and nutrients, ocean chlorofluorocarbons, ocean circulation change, ocean mixing

■ **Abstract** Global ship-based programs, with highly accurate, full water-column physical and biogeochemical observations repeated decadally since the 1970s, provide a crucial resource for documenting ocean change. The ocean, a central component of Earth's climate system, is taking up most of Earth's excess anthropogenic heat, with about 19% of this excess in the abyssal ocean beneath 2,000 m, dominated by Southern Ocean warming. The ocean also has taken up about 27% of anthropogenic carbon, resulting in acidification of the upper ocean. Increased stratification has resulted in a decline in oxygen and increase in nutrients in the Northern Hemisphere thermocline and an expansion of tropical oxygen minimum zones. Southern Hemisphere thermocline oxygen increased in the 2000s owing to stronger wind forcing and ventilation.

The most recent decade of global hydrography has mapped dissolved organic carbon, a large, bioactive reservoir, for the first time and quantified its contribution to export production (~20%) and deep-ocean oxygen utilization. Ship-based measurements also show that vertical diffusivity increases from a minimum in the thermocline to a maximum within the bottom 1,500 m, shifting our physical paradigm of the ocean's overturning circulation.

1. INTRODUCTION

The ocean is variable on all temporal and spatial scales. This variability has both natural and anthropogenic causes. For climate variability and climate change, the global ocean, through its full depth, is singularly important for its role in heat storage and mediation of increasing anthropogenic CO_2 (C_{ant}) in the atmosphere. Single-point time-series stations have increased understanding of the patterns of temporal variability, but by their nature remain limited in the spatial domain. Satellite observations provide global coverage at relatively high temporal resolution, but are restricted to a few surface parameters. Autonomous floats have begun to provide nearly global coverage of temperature and salinity at ten-day intervals, but are currently limited to the upper 2,000 m (Roemmich et al. 2015). A ship-based observing system is the only technique at present for obtaining the necessary highly accurate measurements of physical and biogeochemical properties of the ocean, including carbon.

The Global Ocean Ship-based Hydrographic Investigations Program (GO-SHIP; http://www.go-ship.org) is a systematic reoccupation of select hydrographic sections (see map in **Supplemental Figure 1**, included in Supplemental Appendix 1; follow the Supplemental Materials link from the Annual Reviews home page at http://www.annualreviews.org) with the goal of obtaining full-depth water column measurements of physical and chemical variables (see Supplemental Appendix 1). This program is a component of the Global Climate Observing System (GCOS) and Global Ocean Observing System (GOOS).

Beginning with a comparison of two pairs of zonal hydrographic sections taken some 25 years apart in the North Atlantic (Roemmich & Wunsch 1984), there has been ongoing documentation of the changing properties of the ocean, from the surface to the bottom. In combination with efforts from previous decades, the data emerging from the decadal GO-SHIP program have led to major scientific discoveries that have advanced our understanding of the roles of the ocean in climate change, carbon cycling, and biogeochemical responses to climate change. The GO-SHIP results outlined herein have been key in studies of (*a*) heat and freshwater storage and flux (Section 2), (*b*) circulation changes and mixing (Section 3), (*c*) sequestration of anthropogenic carbon and biogeochemical changes (Section 4), (*d*) ventilation of deep and shallow water masses (Section 5), (*e*) oxygen and nutrient changes (Section 6); and have provided accurate data for (*f*) model calibration and validation, and (*g*) calibration and checks of autonomous sensors.

2. HEAT AND SALINITY

The ocean plays a primary role in taking up and storing heat on our planet. Temporal and spatial variability in ocean heat storage is linked to decadally varying atmospheric forcing and to the spatial pattern and variability of the ocean's overturning circulation (see Section 3). As a result of increases in anthropogenic greenhouse gases, Earth's energy budget is currently not in balance, with more energy being absorbed than returned to space.

Quantifying the planetary energy imbalance is an important part of the projections of how much and how fast the atmosphere will warm (e.g., Frölicher et al. 2014) and anchors satellite measurements of the top-of-the-atmosphere energy imbalance (Loeb et al. 2012). Rhein et al. (2013) estimated that ocean warming took up 93% of that energy imbalance from 1971 to 2010, with 3% each going into melting ice and warming the continents and only 1% going into warming the atmosphere. The significance of the amount of heat stored in the deep ocean has become increasingly evident in the past several years (Purkey & Johnson 2010, Mauritzen et al. 2012). Although the upper ocean has taken up most of the excess heat, approximately 19% has gone into the deep ocean (>2,000 m).

Changes in Earth's heat balance are accompanied by changes in its water cycle. The ocean comprises 70% of the planet's surface; most evaporation and precipitation occurs over the oceans. Seawater is a combination of freshwater and dissolved salts. The salts arise principally from weathering, and the total amount in the ocean has been effectively constant over millions of years. Therefore, ocean salinity, which is proportional to mass of salt per mass of seawater, is principally a measure of dilution of the salts by freshwater.

The ocean salinity distribution is set by the transport of freshwater through the atmosphere and ocean (e.g. Talley 2008). Variation in the hydrological cycle (evaporation, rainfall, and river discharge) and in the cryosphere (e.g., sea ice, glaciers, and ice sheets) is the principal cause for large-scale salinity change. The ocean is effectively a global rain gauge because it covers so much of Earth. A global assessment of changes in freshwater storage using several decades of hydrographic data has shown coherent large-scale patterns (Boyer et al. 2005, Bindoff et al. 2007). This signal has been more clearly delineated by adding data from the upper-ocean Argo profiling float network of the 2000s (Durack & Wijffels 2010). These changes are consistent with increased loss of freshwater from regions of net evaporation (midlatitudes) and its deposition in regions of net precipitation (higher latitudes). Furthermore, a zonal redistribution of freshwater from the saline Atlantic and Indian Oceans to the fresher Pacific has been documented (Bindoff et al. 2007, Durack et al. 2012). These are patterns expected in a warming climate (Rhein et al. 2013).

In the following sections, we focus on temperature and salinity changes in the deep ocean (>2,000 m) because these have been observable only through the use of multidecadal repeat hydrography data. Changes in temperature and salinity in the abyssal ocean are a significant fraction of the overall changes and result from changes in ventilation rates and properties of the waters that fill much of the deep global ocean (e.g., Johnson 2008). Temperature and salinity changes contribute to global and regional sea level rise through thermal expansion and haline contraction, and again, the contribution of the abyssal ocean is not negligible (Kouketsu et al. 2011, Purkey & Johnson 2013).

2.1. Deep-Ocean Warming

GO-SHIP has revealed prominent warming in abyssal waters around the globe (**Figure 1*a***). The strongest warming is observed in the Southern Ocean near the source of Antarctic Bottom Water (Purkey & Johnson 2010). When integrated

globally, the abyssal temperature increase of approximately 0.03°C decade^{-1} in the deep basins around Antarctica amounts to ~ 35-TW rate of warming below 2,000 m between the 1990s and 2000s. This is ~19% of the rate of warming of the entire climate system, which has been estimated as ~183 TW between 1972 and 2008 (Church et al. 2011).

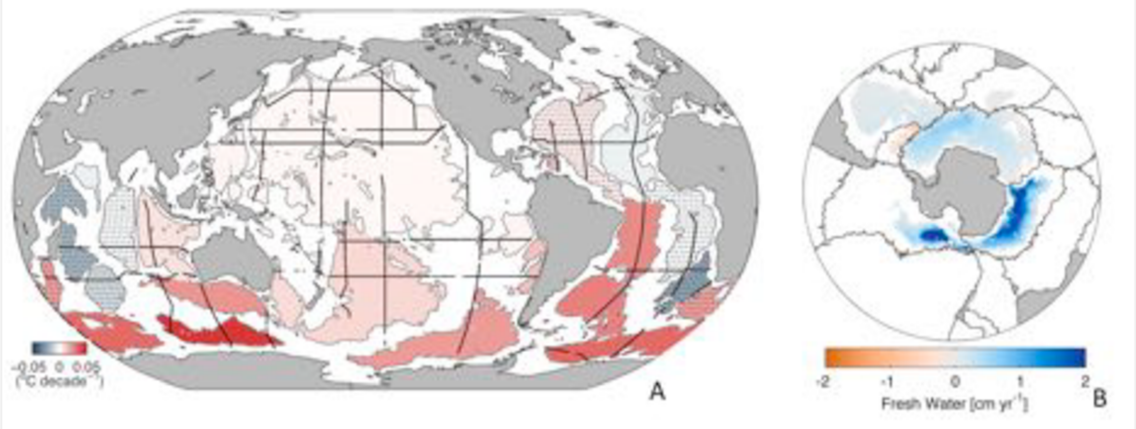

Figure 1 (*a*) Mean warming rates (°C per decade) below 4000 m (color bar) estimated for deep ocean basins (thin gray outlines), centered on 1992–2005. Stippled basin warming rates are not significantly different from zero at 95% confidence. The positions of the repeat oceanographic transects from which these warming rates are estimated (thick black lines) also shown. (Data from Purkey & Johnson 2010.) (Adapted from Rhein et al. 2013) (*b*) Rates of freshwater inventory change (*colors*) resulting from water-mass (θ-S) changes within the Antarctic Bottom Water (θ < 0°C) in deep basins (*areas outlined in thin gray lines*), again estimated from repeat hydrographic sections, where θ is potential temperature and S is salinity. Abbreviations: CLIVAR, Climate Variability and Predictability Program; GO-SHIP, Global Ocean Ship-Based Hydrographic Investigations Program; WOCE, World Ocean Circulation Experiment. Panel *a* adapted from Rhein et al. (2013), based on Purkey & Johnson (2010); panel *b* adapted from from Purkey & Johnson (2013).

Regionally, warming has been strongest in the deep western boundary currents (Kouketsu et al. 2011, Sloyan et al. 2013) and more generally in the western regions of the basins. In the North Atlantic this pattern may be reversed, with warming on the western flank of the Mid-Atlantic Ridge (Johnson et al. 2008). Both patterns may imply a slowdown in the northward flow of abyssal water from Antarctica, as discussed in Section 3.1. A third set of occupations of these sections, starting in 2012, has allowed quantification of deep-ocean changes over longer time periods, such as the abyssal warming in the Brazil Basin observed from 1989 to 2014 (Johnson et al. 2014).

2.2. Deep-Ocean Salinity and Freshwater Changes

GO-SHIP repeat hydrography has enabled the full geographic and depth dependence of salinity changes to be observed. Salinity has increased in the subtropical salinity maxima of the South Indian and South Atlantic Oceans. Near-surface freshening has occurred in the Pacific subtropical salinity maxima (Nakano et al. 2015) and throughout the tropical Atlantic surface waters. The Southern Hemisphere pycnocline, at levels shallower than the Antarctic Intermediate Water, has freshened (Talley 2009, Helm et al. 2010). Oxygen and chlorofluorocarbon (CFC) changes at the same locations (see Sections 5 and 6.1) indicate that this thermocline freshening is likely related to increased ventilation from the south.

Deep salinity changes reflect changes in deep- and bottom-water formation rates and properties, and, like temperature, they can affect sea level through changes in density. In the Southern Hemisphere, freshening of bottom waters throughout the Ross Sea and Adélie Land sectors has been observed from the 1990s through the 2000s, whereas the Weddell Sea salinity has changed very little (**Figure 1*b***). The overall abyssal freshening for the Antarctic Bottom Water of potential temperature $\theta < 0°C$ is equivalent to the addition of approximately 100 Gt $year^{-1}$ [a rate of ~ 0.003 sverdrups (Sv); 1 Gt = 10^{12} kg, and 1 Sv = 10^{9} kg s^{-1}] of freshwater (Purkey & Johnson 2013. This amount is a significant fraction of the increase in ice-sheet melt in recent years (e.g., Rignot et al. 2008). The two changes may be related, with the ice melt freshening shelf waters that are a component of these bottom waters (e.g., Jacobs & Giulivi 2010). Bottom-water salinity decreased by as much as 0.06 (on the PSS-78 scale between 1992 and 2011 in the Ross Sea Bottom Water adjacent to the continental rise, with a smaller decrease offshore (Swift & Orsi 2012). Similar freshening occurred—again, most strongly in the newly formed bottom waters—from 1970 through 2012 offshore of the Adélie Lands to the west (Katsumata et al. 2015).

Repeat hydrography has also revealed decadal variability in the salinity of the various components of the North Atlantic Deep Water (Yashayaev 2007), extending much deeper than the 2,000-m reach of Argo profiling floats, and often partly compensating for the effect of temperature variations on density (and hence sea level) in this region. The shallower anomalies are linked to variations in the strength of winter convection and Labrador Sea Water formation associated with changes in the North Atlantic Oscillation. Below 2,000 m, observed decadal changes in the deep waters fed by the Iceland-Scotland Overflow are likely linked to changes in the properties and amount of Labrador Sea Water that is entrained during the turbulent overflow process, whereas the observed near-bottom Denmark Strait Overflow water variations are strongly interannual.

3. CIRCULATION AND DIFFUSIVITIES

The ocean circulation moves water thousands of kilometers horizontally, carrying heat, salt, freshwater, carbon, and nutrients. Within ocean basins, these wind-driven circulations comprise the Gulf Stream and Kuroshio gyre systems of the North Atlantic and North Pacific and their counterparts in the Southern Hemisphere, namely the Brazil, Agulhas, and East Australian Current systems. The eastward-

flowing Antarctic Circumpolar Current system encircles Antarctica, connecting the ocean basins and their water properties.

Connected with this horizontal circulation is the ocean's overturning circulation, which involves changes in the depth and density of water parcels. Much of the change in density occurs at the surface, resulting from net heat and freshwater exchange with the atmosphere combined with vigorous vertical and lateral mixing with adjacent waters. Below the surface mixed layer, motion is approximately along surfaces of constant density (isopycnals), but slow mixing within the stratified ocean interior gradually modifies water properties, including density; on a large scale, water parcels drift across isopycnals. Because the maximum density of a water parcel tends to be close to its density when it leaves the mixed layer, the overturning circulations associated with tropical and subtropical gyres are relatively shallow. Waters below the pycnocline are ventilated from high latitudes. Deep waters are distributed globally by a horizontal circulation in which deep western boundary currents are prominent.

GO-SHIP and its predecessors are the principal source of information about changes in the shallow and deep overturning circulations. GO-SHIP observes chemical properties associated with upper ocean ventilation (see Sections 5 and 6) and it measures changes in abyssal properties and water transports (described next).

3.1. Abyssal Ocean Circulation Changes

Abyssal and deep flows are a major component of the global overturning circulation (Lumpkin & Speer 2007, Talley 2013). The deep warming discussed in Section 2.1 corresponds to a contraction rate of ~8 Sv for Antarctic Bottom Water of $\theta < 0°C$ (Purkey & Johnson 2012). A reduction in CFC inventories in the abyssal waters of the Weddell Sea (Huhn et al. 2013) suggests a significant decrease in ventilation rates in at least that sector of the Southern Ocean.

This decline in Antarctic Bottom Water volumes (roughly a descent of $\theta = 0°C$ at approximately 100 m decade^{-1}) appears to be associated with a reduction in northward flows of slightly warmer Lower Circumpolar Deep Water from the Southern Ocean through the South Pacific and South Atlantic (Kouketsu et al. 2011). The assimilation of repeat hydrographic section data into a general circulation model by these investigators yielded a slowdown in the northward transport of bottom waters of 0.7 Sv decade^{-1} in the South Pacific and 0.4 Sv decade^{-1} in the western South Atlantic from 1968 to 2005. The abyssal warming pattern in the South Pacific, with more warming at the western boundary (Sloyan et al. 2013), is consistent with a reduced eastward pressure gradient force near the bottom, and hence with reduced geostrophic northward flow. (The geostrophic balance, between the pressure gradient force and the Coriolis force, dominates ocean currents.)

In the North Pacific, an inverse model analysis using repeat hydrography data from 1985 and 2005 suggested a decrease of 1.5 Sv in northward transport of bottom waters of Southern Ocean derivation (Kouketsu et al. 2009). In the North Atlantic, analysis of five sections across 24°N occupied between 1981 and 2010 suggested that northward flow of bottom waters derived from Southern Ocean Lower Circumpolar Deep Water is reduced by order 1 Sv, although not monotonically

(Frajka-Williams et al. 2011). This reduction of bottom-intensified northward flow over the Mid-Atlantic Ridge is consistent, again through geostrophic balance, with the deep pattern of warming on the western flank of the Mid-Atlantic Ridge and cooling to the west (Johnson et al. 2008).

Whereas advection of changes in the Lower Circumpolar Deep Water in the Northern Hemisphere would take many decades, perhaps centuries, to be measurable in temperature and salinity, planetary waves can carry signatures of such changes all the way to the North Pacific in a few decades, as demonstrated by analysis of a global data assimilation of repeat hydrographic data (Masuda et al. 2010). Indeed, the highly accurate GO-SHIP measurements have shown a slight warming in very old bottom waters in the far northern Pacific (Fukasawa et al. 2004), which was attributed to this wave mechanism.

3.2. Transport Analyses and Changes

Measuring changes in ocean circulation, and the consequences of those changes for Earth's heat and carbon budgets, is difficult; currents are highly variable on a broad range of temporal and spatial scales. Transport across hydrographic sections can be estimated using a combination of direct measurements of currents and geostrophic calculations based on the density field. More robust estimates can be made by using the hydrographic and current measurements in inverse models. GO-SHIP's synoptic, decadal sampling is complemented by data sets with more frequent sampling and with more uniform spatial coverage, such as sea surface height from satellite altimetry and Argo float velocity (e.g., Roemmich et al. 2007) or resource-intensive boundary current transport and midocean arrays (e.g., Carton & Hakkinen 2011) that provide direct velocity estimates. Ocean state estimations incorporating all of these available data sets are becoming useful circulation analysis tools (Katsumata & Masuda 2013, Wunsch & Heimbach 2013).

In the Southern Hemisphere, hydrographic section transports and properties indicate that the subtropical gyre circulations in the Indian and Pacific Oceans strengthened from the 1990s to the mid-2000s. Palmer et al. (2004) documented subtropical gyre strengthening in the Indian Ocean from 1987 to 2002 using repeats of the 32°S section. This finding was consistent with the observed signature of increased ventilation: increasing oxygen in the thermocline (McDonagh et al. 2005) and changes in upper-ocean temperature and salinity, notably in the thick mode-water layer (Bryden et al. 2003). Roemmich et al. (2007) demonstrated spin-up in the South Pacific subtropical gyre using a combination of changes in sea surface height from satellite altimetry, mid-depth velocity field from Argo floats, and thermocline pressure gradient from repeated hydrographic data, in this case from a meridional section at 170°W that showed changes in the meridional gradient of surface dynamic height and thermocline depth. The strengthening was associated with increased westerly winds and stronger Ekman convergence, associated with an increasing Southern Annular Mode index (Thompson et al. 2000).

As part of the deep overturn of the global circulation, the Atlantic Meridional Overturning Circulation has been of interest for several decades. For a review of the

increasingly robust indications of a mild decrease in its strength, see the sidebar, The Slowing of the Atlantic Meridional Overturning Circulation.

THE SLOWING OF THE ATLANTIC MERIDIONAL OVERTURNING CIRCULATION

The Atlantic Meridional Overturning Circulation (AMOC) transports warm upper-ocean waters northward where they are cool in large heat-loss regions of the North Atlantic and Nordic Seas, then returned southward as cold North Atlantic Deep Water. This results in a large northward heat transport across the full length of the Atlantic. Climate models project an anthropogenic decrease in AMOC strength caused by increasing stratification in the north (**Carton et al. 2014**). **Bryden et al. (2005)** reported decreasing AMOC strength since the 1950s using hydrographic sections at 24–26°N repeated over several decades, but seasonally biased to summer. There is evidence for continued decline through 2011 (Hernández-Guerra et al. 2014). Direct measurements of the AMOC since 2004 have shown large seasonal and interannual variability but also a small decrease from 2004 to 2012 (**Rayner et al. 2011**, **McCarthy et al. 2015**) that is seen in a historical reconstruction of the AMOC from 1980 to 2005 based on data from hydrographic stations (**Longworth et al. 2011**). Using paleo-reconstructions, **Rahmstorf et al. (2015)** suggested that this recent decline is part of both decadal-scale variability and a trend going back to at least the 1930s, and likely as far back as the 1800s. Taken together, these results suggest that the AMOC is indeed slightly slowing.

The meridional overturning circulation strength in the Indian and Pacific Oceans is measured by the net northward transport in the deepest layers, which therefore warms, upwells diapycnally, and returns southward at a lower densities. For the meridional overturning circulation in the Southern Hemisphere Indian Ocean, the difference in transport assessed from the same 32°S 1987–2002 repeats was within the large range of uncertainty, based on geostrophic calculations from the CTD (conductivity, temperature, and depth) profiles using lowered acoustic Doppler current profiler (LADCP) velocities as an initial reference for the 2002 section (McDonagh et al. 2008).

Katsumata & Masuda (2013) used Southern Ocean repeat sections in the 1990s and 2000s and direct velocity measurements from Argo float drift in a box inverse model to estimate the Southern Ocean circulation and compare it with ocean general circulation models. They found that the meridional overturning circulation strength as measured by the northward transport of the bottom water decreased in the ocean models, which was consistent with the inverse box model, within the uncertainties. Part of the weakening is explained by the deep warming discussed in Section 3.1. By contrast, a comparison of hydrographic data from the World Ocean Circulation Experiment (WOCE) in the 1990s with those from GO-SHIP in the 2000s indicated that the transport of the eastward Antarctic Circumpolar Current has not significantly changed despite several decades of strengthening westerly winds (e.g., increase in the Southern Annular Mode index) (Katsumata & Masuda 2013.

3.3. Ocean Mixing and Vertical Diffusivity

The ocean's vertical and lateral distributions of heat, salt, and tracers are maintained not only by advection from source regions but also by ocean mixing, both across isopycnals (diapycnal) and along isopycnals. Such ocean mixing has been the focus of the Climate Variability and Predictability (CLIVAR) program's Diapycnal and Isopycnal Mixing Experiment in the Southern Ocean (DIMES) (LaCasce et al. 2014) and is not summarized here. Closing the ocean's overturning circulation requires diapycnal mixing to flux heat and buoyancy downward, reducing the density of deep waters as they gradually move upward (e.g., Munk 1966, Sloyan & Rintoul 2001, Talley 2013). Space- and time-averaged diapycnal transports associated with the ocean's large-scale overturning circulation may be diagnosed from basin-scale heat, salt, and tracer budgets using hydrographic sections, yielding estimates of diapycnal diffusivity (e.g., Ganachaud & Wunsch 2000, Lumpkin & Speer 2007, Macdonald et al. 2009, Huussen et al. 2012).

Direct observations of diapycnal diffusivity from microstructure measurements, which are rare, have been essential for deriving a finestructure parameterization of dissipation and diffusivity (Gregg 1989, Polzin et al. 1995, Gregg et al. 2003). With this parameterization, spatial patterns of mixing can be estimated from the much more numerous CTD and LADCP profiles, such as those collected by GO-SHIP. The relationship between internal-wave shear/strain and turbulence presumes a cascade of energy from longer to shorter internal waves and turbulence (Henyey et al. 1986). In dynamically quiet regions away from boundaries and strong currents, finestructure parameterizations are accurate to within approximately a factor of two (Polzin et al. 2014, Whalen et al. 2015). Regional and global patterns of turbulence and mixing have been mapped (e.g., Naveira Garabato et al. 2004, Sloyan 2005, Kunze et al. 2006, Whalen et al. 2012).

A significant finding is that in most ocean basins the vertical distribution of diapycnal diffusivity and dissipation has two maxima (e.g., **Supplemental Figure 2**, included in Supplemental Appendix 2 along with all subsequent supplemental figures): one in the upper ocean (200–1,000 m) and one within 1,500 m of the seafloor (Kunze et al. 2006, Huussen et al. 2012, Waterhouse et al. 2014). Diffusivities are low ($<10^{-5}$ m^2 s^{-2}) in large regions of the ocean's thermocline.

Diapycnal diffusivity is consistently high (>10^{-4} m^2 s^{-2}) over areas with rough topography, where breaking internal waves (driven by tidal and other forces, including deep strong currents) cause turbulence, as well as in regions of high kinetic energy.

Quantitative comparisons between the diapycnal transport and observed mixing are, however, not yet satisfactory (Huussen et al. 2012). It is possible that mixing near topography has been underestimated and that, while results from the finestructure parameterization suggest enhanced vertical structure in the equatorial band, the parameterization is likely inaccurate because of the very different nature of internal waves and vertical shear there (Whalen et al. 2012).

These results from finestructure parameterization methods applied to temperature-salinity profile data, including those collected in GO-SHIP, are contributing to new parameterizations of mixing in global-scale ocean circulation models (Decloedt & Luther 2012, Melet et al. 2013). The structure of mixing can affect the nature of deep circulation, deep overturning, and water properties from the thermocline to the abyss, and hence accurate parameterization can affect the ability of ocean models to capture the response to changing surface forcing.

4. CARBON

4.1. Inorganic Carbon Inventories and Fluxes

The global ocean has continued to take up a substantial fraction of the C_{ant} emissions from fossil fuel combustion and net land-use change since the 1990s, and it is therefore a major mediator of global climate change. General ocean circulation models and data-constrained models suggest that the ocean absorbed approximately 37 Pg C of C_{ant} between 1994 and 2010 (Khatiwala et al. 2013) (**Figure 2**), increasing the C_{ant} inventory from 118 ± 20 Pg C to 155 ± 31 Pg C. This amounts to a mean annual uptake rate of approximately 2.3 Pg C $year^{-1}$, or approximately 27% of the total C_{ant} emissions over this time period. However, this globally critical estimate is based on numerical techniques using transient tracers and has not been independently verified using ocean carbon observations. The sustained repeated occupations of many of the lines measured during the 1990s and 2000s provide an observation-based uptake estimate.

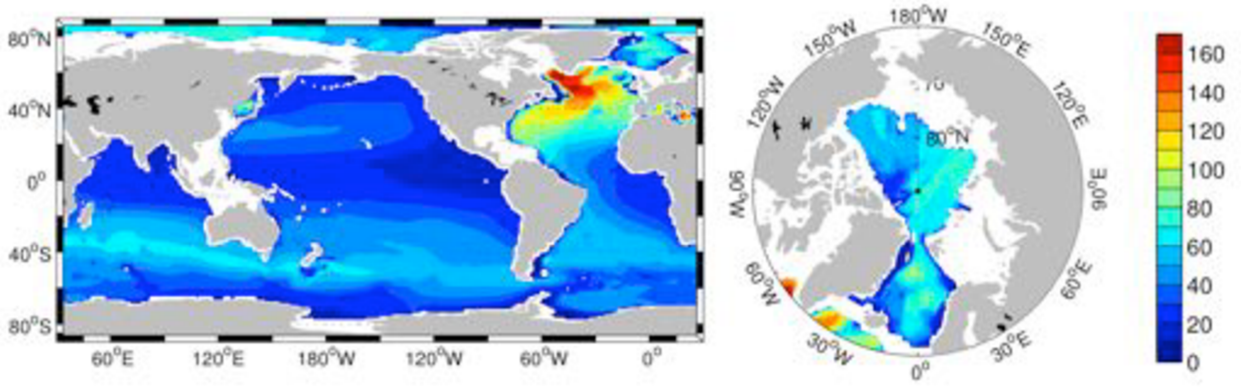

Figure 2 Compilation of 2010 column inventories (summed vertically over the full water column) of C_{ant}. Excluding the marginal seas, the global ocean inventory is 150 ± 26 Pg C. Abbreviation: C_{ant}, anthropogenic CO_2. From Khatiwala et al. (2013)**.**

Changes in dissolved inorganic carbon (DIC) concentration between repeat occupations reflect both anthropogenic C_{ant} uptake as well as natural variations in circulation and organic matter remineralization (e.g., Sabine & Tanhua 2010). Several methods have been developed and tested to accomplish this separation along repeat sections, including the extended multilinear regression method (EMLR) (Friis et al. 2005), which has recently been modified to permit basin-wide estimates of C_{ant} trends by utilizing data from repeat occupations and climatological data from the *World Ocean Atlas 2013* (Locarnini et al 2013, Zweng et al 2013) (D. Clement & N. Gruber, personal communication).

Preliminary global-scale results from this modified EMLR indicate a C_{ant} uptake rate of approximately 2.6 Pg C $year^{-1}$ (1994–2006), i.e., slightly above the model-based estimate of 2.3 Pg C $year^{-1}$ (Khatiwala et al. 2013). However, the large uncertainty of this preliminary estimate (±0.5 Pg C $year^{-1}$) precludes any statement about the significance of this difference. Using observational data and the ΔC* method of Gruber et al. (1996), Kouketsu & Murata (2014) estimated an even higher storage rate of 2.9 ± 0.4 Pg C $year^{-1}$ for the most recent decade. Takatani et al. (2014) used the GO-SHIP reference and high-frequency sections to show that the rate of C_{ant} increase on isopycnals in the western North Pacific subtropical gyre over the past two decades is consistent, within the observational uncertainty, with that expected from the atmospheric CO_2 increase, Revelle factor, and CFC age (see Setion 5.1 and **Supplemental Figure 6** below). The mean rate of C_{ant} inventory change over the past few decades varies from 0.22 ± 0.05 mol m^{-2} $year^{-1}$ to 0.94 ± 0.10 mol m^{-2} $year^{-1}$, depending on the depth to which the ocean is ventilated. (For comparison, the 2.3 to 2.9 Pg C $year^{-1}$ global mean storage rate quoted above corresponds to 0.53 to 0.67 mol m^{-2} $year^{-1}$.)

The C_{ant} column inventory has substantial spatial variation, with the total water column inventory in **Figure 2** dominated by upper ocean ventilation patterns. The South Pacific has higher C_{ant} storage rates than the North Pacific (Murata et al. 2007,

Sabine et al. 2008). In the Indian Ocean, C_{ant} storage rates are largest south of the equator, where C_{ant} increases have been observed to 1,800 m (Murata et al. 2010). Several studies that used observations from hydrographic sections have indicated that the Southern Ocean may be responsible for as much as 30–40% of the global C_{ant} uptake (e.g., Gruber et al. 2009, Khatiwala et al. 2009). There is still debate about whether this uptake is stored or exported (Sabine et al. 2004, van Heuven et al. 2011) and what water masses are involved (e.g., Gruber et al. 1996, Sabine et al. 2004, van Heuven et al. 2011, Pardo et al. 2014). Researchers are using both carbon parameters and other tracers (e.g., CFCs, CCl_4, and ^{39}Ar) from these cruises to investigate the possibilities. Deep western boundary currents serve as important ventilation pathways and carry an appreciable amount of anthropogenic carbon into the interior. The western basins of the North and South Atlantic and North Pacific show significantly higher C_{ant} inventories and storage rates than the eastern basins (Körtzinger et al. 1999, Murata et al. 2008, Brown et al. 2010, Waters et al. 2011).

Substantial temporal differences in C_{ant} storage rates have been observed on decadal and subdecadal timescales (Sabine & Tanhua 2010; Wanninkhof et al. 2010, 2013a; Khatiwala et al. 2013; Tanhua et al. 2013a) (**Figure 3**). Temporal variability in C_{ant} of similar magnitude and pattern also occurs in numerical simulations, highlighting the need to integrate repeat section occupations with other data and model information (Levine et al. 2008). Pérez et al. (2010) found that the C_{ant} storage rate in the North Atlantic was dependent on the North Atlantic Oscillation, with the highest C_{ant} storage rates occurring during the positive phase of this oscillation, consistent with model studies linking North Atlantic Oscillation–driven increases in mode-water formation to enhanced transport of C_{ant} from surface water into the ocean interior (Levine et al. 2011). Furthermore, Pérez et al. (2013) showed a decrease in uptake from 1990 to 2006 that they attributed to a weakening of the meridional overturning circulation.

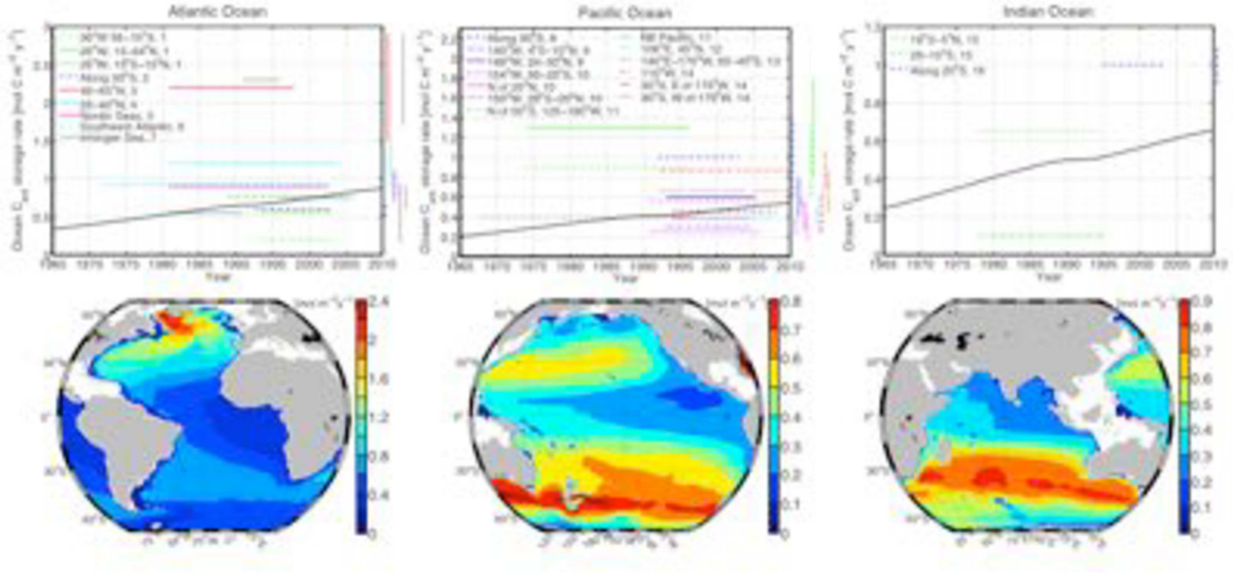

Figure 3 Decadal storage rates of C_{ant} as observed from repeat hydrography cruises. (*a*) Measurement intervals bracketed by repeat hydrography cruises in the Northern Hemisphere (*solid lines*), tropics (*dash-dotted lines*), and Southern Hemisphere (*dashed lines*); each color denotes a different study. Estimates of uncertainties are shown as vertical bars with matching colors along the right axes. The solid black lines represent the basin average storage rates using Green's functions. (*b*) Maps of decadal storage rates from a Green's function inversion averaged over 1980–2005 using data shown in panel *a*; note that the color scales differ in each subpanel. Abbreviation: C_{ant}, anthropogenic CO_2. Figure adapted from Khatiwala et al. (2013).

Ocean interior carbon observations also provide a constraint on decadal average net sea-air CO_2 flux of both natural CO_2 and C_{ant} through ocean inversion procedures, provided one knows the ocean's circulation and mixing well (Gloor et al. 2003). Using an ensemble of ten general circulation models and inorganic carbon data from the 1990s and 2000s, including GO-SHIP, Gruber et al. (2009) estimated the net sea-air flux of CO_2 over 23 regions globally (**Supplemental Figure 3**). They found a remarkable level of agreement with sea-air CO_2 fluxes inferred from surface-ocean pCO_2 measurements (Takahashi et al. 2009) at a regional level, with differences rarely exceeding 0.1 Pg C year^{-1}. The C_{ant} uptake was estimated to be 2.2 ± 0.3 Pg C year^{-1}, consistent with but slightly higher than the estimate based on surface sea-air CO_2 fluxes (Takahashi et al. 2009, Wanninkhof et al. 2013b, Landschützer et al. 2014).

The uptake of C_{ant} from the atmosphere into the ocean interior has also resulted in ocean acidification—a long-term decrease in pH since the beginning of the industrial era of up to 0.1 in surface waters (e.g., Feely et al. 2009). Feely et al. (2004) showed how the increased CO_2 reduced the aragonite and calcite saturation state of the global ocean. This effect of elevated atmospheric CO_2 has been illuminated by results from GO-SHIP and the earlier hydrographic sampling programs (Feely et al. 2004, 2009; Key et al. 2004; Sabine et al. 2004), showing pH changes in the surface water of approximately −0.002 year^{-1} from 1991 to 2006 along sections in the North Pacific (for a summary, see Rhein et al. 2013). The Global Ocean Data Analysis Project (GLODAP) data product included estimates of the preindustrial DIC concentration derived from differences between the measured DIC and the estimated anthropogenic component. Orr et al. (2005) used these GLODAP estimates for comparison with 13 models in the Ocean-Cycle Model Intercomparison Project (OCMIP-2) to show the anthropogenic reduction in aragonite and calcite saturation, and then as a baseline for 100-year projections in 3 coupled models forced with several Intergovernmental Panel on Climate Change (IPCC) scenarios for rising atmospheric CO_2. Yool et al. (2013a, b) used GLODAP and *World Ocean Atlas 2005* (Antonov et al. 2006, Locarnini et al. 2006) data products to estimate the pH change from the preindustrial to the present (**Supplemental Figure 4**). The smallest pH changes (−0.04 to −0.06) have been in the tropics and subtropics; the greatest (−0.08 to −0.1) have been in the northern North Atlantic and North Pacific and in a circumpolar band in the Southern Ocean. The larger changes result from a

combination of greater C_{ant} invasion, lower buffer capacity, and lower water temperature (Sabine et al. 2004, Feely et al. 2009, Egleston et al 2010).

4.2. Dissolved Organic Carbon

Dissolved organic carbon (DOC) is one of the largest bioreactive pools of carbon in the ocean (Hansell et al. 2009, 2012). Over the past decade, time-series and basin-scale observations (~50,000 data points) have revealed temporal and spatial variability of DOC in unprecedented detail (**Figure 4**); from this detail, the processes controlling the variability can be inferred. The inventory of oceanic DOC is estimated to be ~662 ± 32 Pg C, 200 times the mass of the organic carbon in suspended particles but approximately 1/50th of the total DIC inventory (Hansell et al. 2009).

The bulk DOC pool contains a myriad of compounds that turn over on timescales from seconds to millennia (Hansell et al. 2012, Carlson & Hansell 2015). The majority of the newly produced DOC is rapidly remineralized by heterotrophic bacterioplankton within the ocean's surface layer (Carlson & Hansell 2015). However, ~20% of global net community production (~1.9 Pg C $year^{-1}$) escapes rapid microbial degradation for periods long enough to be exported from the euphotic zone via convective mixing or isopycnal exchange into the ocean's interior (Copin-Montgut & Avril 1993, Carlson et al. 1994, Hansell et al. 2009). DOC export occurs with deep- and mode-water formation in the North Atlantic (**Figure 4**) as midlatitude, warm, DOC-enriched surface waters are transported with surface currents to subpolar and high latitudes. Here, convective overturn transports the DOC deep into the interior, where it is slowly removed through southward flow.

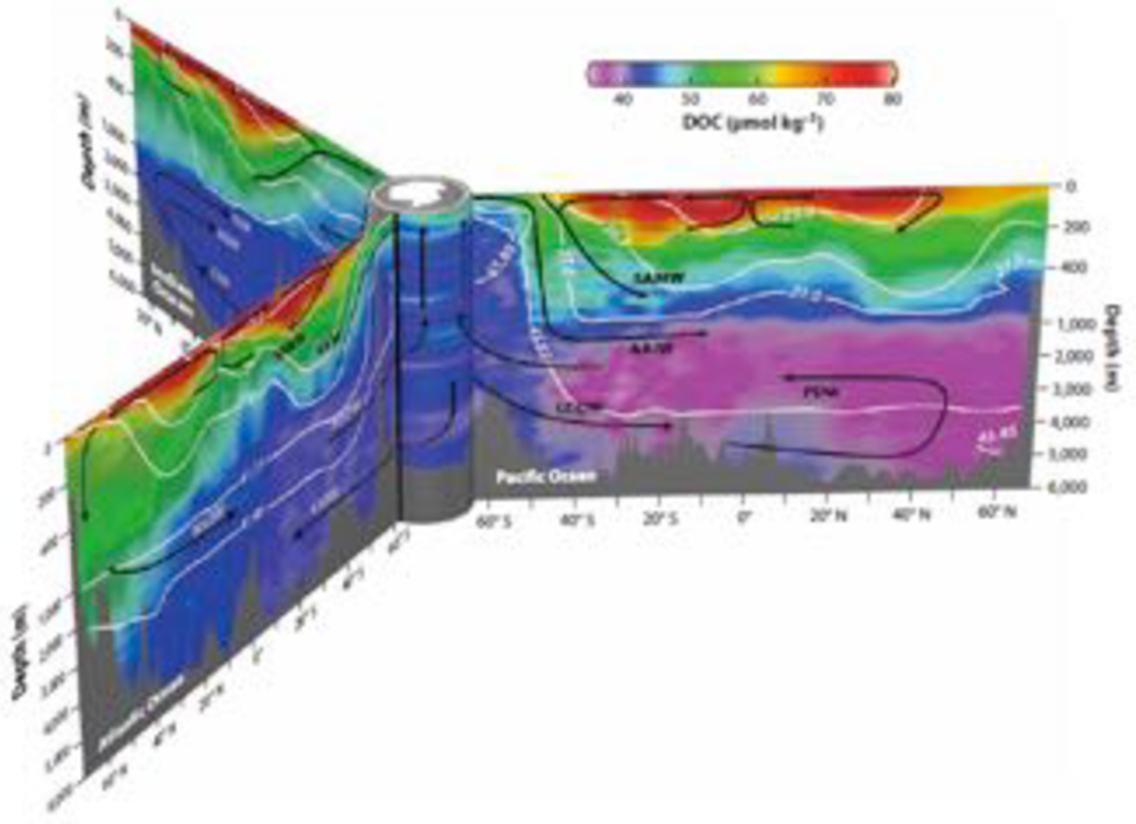

Figure 4 Distributions of DOC in the Atlantic, Pacific, and Indian Oceans on GO-SHIP repeat hydrography lines A16, P16, and I8/I9, respectively, with water from all lines connected via the Antarctic Circumpolar Current. Arrows depict water-mass renewal and circulation; white lines indicate isopycnal surfaces. Note the DOC export in the North Atlantic with North Atlantic Deep Water formation and the subsequent DOC loss during deep circulation to the South Atlantic. In the Pacific, there is a northward invasion of relatively DOC-enriched Circumpolar Deep Water along the bottom, slow removal of DOC into the far North Pacific, and return flow of DOC-impoverished water to the south at mid-depths. Abbreviations: AABW, Antarctic Bottom Water; AAIW, Antarctic Intermediate Water; CDW, Circumpolar Deep Water; DOC, dissolved organic carbon; GO-SHIP, Global Ocean Ship-Based Hydrographic Investigations Program; IODW, Indian Ocean Deep Water; IOIW, Indian Ocean Intermediate Water; LCDW, Lower Circumpolar Deep Water; NADW, North Atlantic Deep Water; PDW, Pacific Deep Water; SAMW, Subantarctic Mode Water. Figure adapted from Figure 2 in Hansell et al. (2009).

Previously, estimating the removal rates of exported DOC within the ocean's interior was not possible owing to the slow decay rates of the biologically recalcitrant DOC. However, coupled measures of bulk DOC, DOC characterization, water-mass age tracers, and other biogeochemical variables (Hansell et al. 2009, 2012; Carlson et al. 2010; Goldberg et al. 2011) obtained by GO-SHIP have greatly improved understanding of bulk DOC distribution, fractions of DOC lability, and DOC export (Hansell et al. 2012, Hansell 2013). For example, linear and multiple

linear regression models applied to pairwise measurements of DOC and CFC-12 ventilation age retrieved from major water masses within the main thermocline and North Atlantic Deep Water (lines A16, A20, and A22) allow estimates of decay rates for exported DOC ranging from 0.13 to 0.94 μmol kg^{-1} $year^{-1}$, with higher DOC concentrations driving higher rates. A comparison of the change in DOC with the change in oxygen in the same water masses suggested that DOC oxidation contributes 5–29% of the apparent oxygen utilization in the deep water masses of the North Atlantic (Arístegui et al. 2002, Carlson et al. 2010).

Measurements of carbohydrate and dissolved combined neutral sugar concentrations allow further assessment of changes in chemical character along meridional transects in the North Atlantic (A20) and South Pacific (P16S). As microbes remineralize dissolved organic matter (DOM), they preferentially remove the most labile components of DOM, such as carbohydrates and dissolved combined neutral sugars, leaving behind more recalcitrant components. Survey data of these components demonstrate systematic diagenetic patterns across ocean basins (Goldberg et al. 2011), providing further insight into the roles that stratification, ventilation, export, and subsequent remineralization play in DOM quality. For example, meridional transects in the South Pacific and North Atlantic reveal a common diagenetic trajectory in the surface 300-m along which glucose becomes enriched relative to mannose and galactose as DOM is degraded. Departure from this trajectory within the euphotic zone could indicate recently-produced "bloom" DOM, while departure in the mesopelagic zone could indicate recently exported DOM (Goldberg et al., 2011). The compositional data together with bulk DOM dynamics provides important important information about DOM production, consumption, and its transformation.

5. OCEAN VENTILATION: TRANSIENT TRACERS

5.1. Chlorofluorocarbons, SF_6, and Tritium-^{3}He

Anthropogenic transient-tracer distributions provide insight into the pathways, rates, and temporal variations in the processes ventilating the ocean on decadal timescales (Johnson et al. 2008, Wanninkhof et al. 2013b). CFCs, sulfur hexafluoride (SF_6), and bomb tritium have been entering the ocean since the middle of the twentieth century (**Supplemental Figure 5**), during which time the ocean has taken up approximately two-thirds of its anthropogenic carbon inventory. CFC and tritium-^{3}He data, especially as used with transit time distributions (TTDs; see below), have played a key role in reconstructing the complex spatial and temporal evolution of C_{ant} in the global ocean (Tanhua et al. 2008, Khatiwala et al. 2009, Wanninkhof et al. 2013a, Sabine & Tanhua 2010), estimating apparent oxygen utilization rates (Jenkins 1977; Stanley et al. 2012; Sonnerup et al. 2013, 2015), and separating observed changes in oxygen and nutrients into physical (e.g., solubility, circulation, and mixing) and biological processes (Jenkins 1998; Emerson et al. 2001; Mecking et al. 2006; Sonnerup et al. 2013, 2015). Transient tracers have also been used in testing and evaluating a variety of global ocean circulation and biogeochemical

models (Dutay et al. 2002, Matsumoto et al. 2004, Peacock et al. 2005, Hartin et al. 2014, Long et al. 2013).

Ventilation rates of a water mass can be estimated using transient-tracer-derived ages, which measure the elapsed time since last contact with the surface ocean (see global age maps in **Supplemental Figure 6**). The well-characterized atmospheric histories of the CFCs and SF_6 (Walker et al. 2000, Bullister 2015) along with the solubility of these gases in seawater (Warner & Weiss 1985, Bullister et al. 2002) allow the equilibrium concentrations of these compounds in the surface ocean, and thus newly subducted waters, to be modeled as a function of time (e.g., Tanhua et al. 2013b). The Montreal Protocol on Substances that Deplete the Ozone Layer restricted the production and uses of CFCs beginning in 1989, which resulted in atmospheric CFC-11 and CFC-12 concentrations peaking in the late 1990s and early 2000s, respectively, and then slowly decreasing, whereas SF_6 has been increasing in the atmosphere at 5–7% per year for the past two to three decades (**Supplemental Figure 5**). Decay of tritium to ^{3}He provides an additional radioisotope natural clock for the isolation of water parcels from the atmosphere (Jenkins 1977).

Tracer ages are modified by mixing and complicated by the nonlinear source functions (e.g., Doney et al. 1997, Mecking et al. 2006, Tanhua et al. 2013b, Waugh et al. 2013). A commonly used technique, TTDs, assumes that the tracer age is composed of a spectrum of ages. The addition of SF_6 provides improved estimates of mixing of different water parcels. Two TTD methods have been used: the inverse Gaussian method, which assumes a one-dimensional advection-diffusion process (e.g., Waugh et al. 2003, 2013), and the maximum entropy method, which relaxes this assumption and provides information on water-mass composition as well as ages (Holzer et al. 2010). Both methods can include natural radiocarbon (^{14}C), which provides temporal information for water formed prior to the transient-tracer invasion (see Section 5.2).

The global thermocline is well ventilated on the timescale of the CFC/SF_6 and bomb-tritium transient, whereas deeper isopycnal surfaces are much less ventilated (**Figure 5**, **Supplemental Figure 6**). The CFC-12 decadal differences shown in **Figure 5** show the invasion of the time-dependent signal into the thermocline, with the greatest increases at the front of the pulse of the tracer. Regions of the ocean where *p*CFC ages in the thermocline exceed several decades include the deep portions of oxygen minimum zones and the northern Indian Ocean thermocline. CFC distributions, as presented in the WOCE Hydrographic Program Atlases, reveal well-ventilated deep and bottom waters in the Southern Ocean (Sparrow et al. 2005-2013) and North Atlantic (LeBel et al. 2008).

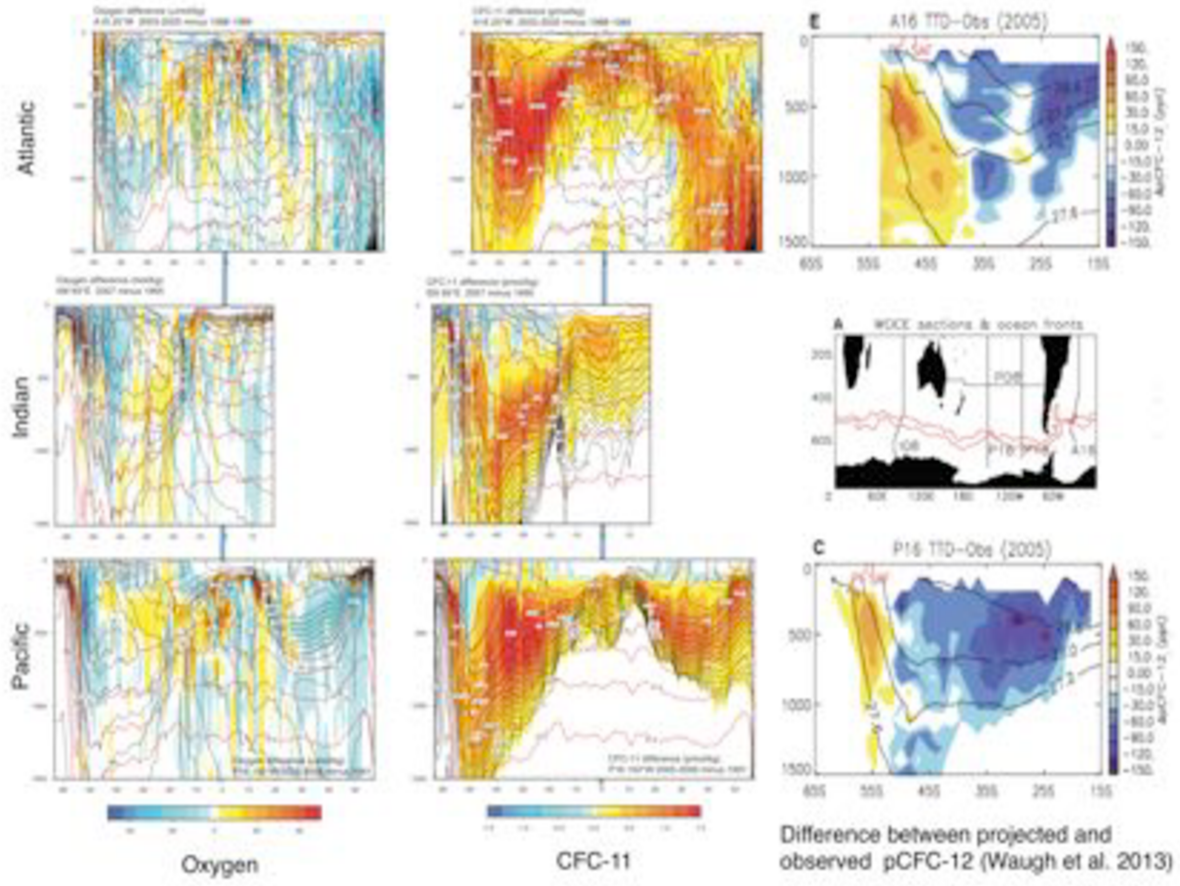

Figure 5 (*a*,*b*) Differences in oxygen (panel *a*) and CFC-11 (panel *b*) between 0 to 1,500 m along three transects: A16 in the Atlantic Ocean along ~20°W (*top*, 2005–2006 minus 1989), I8/I9 in the Indian Ocean along ~95°E (*middle*, 2005 minus 1995), and P16 in the Pacific Ocean along ~150°W (*bottom*, 2005–2006 minus 1991. Supplemental Figure 1 provides a map of the complete A16, I8/I9, and P16 section locations. Properties were interpolated to neutral density surfaces, differenced, and then projected back to depth coordinates, using the neutral density from the earlier year for the projection. Thus, the heave caused by vertical migration of the neutral density surfaces is excluded. Each panel includes overlain contours of neutral density (*red lines*) and of the property itself from the earlier occupation (*black lines*). (*c*) Differences between TTD-predicted and observed *p*CFC-12 for the 2005 cruises compared with those from 1989 (line A16, *top*) and 1991 (line P16, *bottom*). Isopycnals (*black lines*) are from earlier occupations of the A16 and P16 sections. The TTD calculations use $\Delta/\Gamma = 1.0$ and a surface saturation of 90%. Negative values (*blues* and *purples*) mean that there was a higher *p*CFC-12 than expected in the 2005 occupation, indicating younger water or greater ventilation than expected; positive values (*yellows* and *reds*) mean that there was a lower *p*CFC-12 than expected in the 2005 occupation, indicating older water or less ventilation than expected. Abbreviations: CFC,

chlorofluorocarbon; PF, polar front; SAF, subantarctic front; TTD, transit time distribution. Panel *c* adapted from Waugh et al. (2013).

Models of climate change predict that increased stratification should lead to decreased ventilation. Such an effect is seen in the Northern Hemisphere subtropics and subpolar thermoclines and in the Antarctic Circumpolar Current, where predicted CFCs based on TTDs were lower than predicted and oxygen declined (**Figure 5**). However, decadal trends in the subtropical gyres of the Southern Hemisphere indicate increased ventilation for the deep thermocline. The observed increase in CFC-11 and CFC-12 concentrations in the Southern Hemisphere subtropical thermocline compared with those in the 1990s (**Figure 5**) has been greater than predicted by either models or TTDs, and tracer ages have decreased (Fine 2011, Waugh et al. 2013, Fine et al. 2014) (**Figure 5**). Thermocline oxygen increases (McDonagh et al. 2005, Talley 2009, Mecking et al. 2012) (see Section 6.1 and reference to **Supplemental Figure 9** therein) have been associated with increasing ventilation caused by changes in the Southern Annular Mode (Roemmich et al. 2007) that were reflected in increasing CFC concentrations in the lower thermocline (Fine 2011). Both oxygen distributions and TTDs lead to the same conclusion: that ventilation rates in the southern subtropical gyres had been increasing into the 2000s, but this trend has reversed in recent years (see Section 6.1).

Transient-tracer inventory calculations (Smethie & Fine 2001, Orsi et al. 2002, Rhein et al. 2002, Smethie et al. 2007, LeBel et al. 2008) provide integral water-mass formation rates for deep water masses (Hall et al. 2007). As an example, North Atlantic CFC-12 inventory changes over the period 1997–2005 showed a reduction in classical Labrador Sea Water formation (Rhein et al. 2011), whereas upper Labrador Sea Water formation increased (Kieke et al. 2006, 2007). Altimeter analysis showed that decreased classical Labrador Sea Water formation was accompanied by a decreased subpolar gyre transport index (Curry & McCartney 2001, Kieke et al. 2007, Rhein et al. 2011) and decreased strength of the subpolar gyre (Hakkinen & Rhines 2004, Hakkinen et al. 2008). Measurements of CFCs confirm the importance of the deep western boundary current as an advective pathway into the subtropics, and interior CFC concentrations support the importance of interior pathways that are related to the role of eddies and winds (Lozier 2010). This is consistent with tritium-^{3}He data from the Transient Tracers in the Ocean program in the North Atlantic's Deep Western Boundary Current (DWBC) compared with the deep-interior basins east of the DWBC (Doney & Jenkins 1994).

5.2. Radiocarbon

Oceanic ^{14}C is both a transient and a natural tracer that has undergone decadal changes owing to atmospheric nuclear weapons testing in the 1950s and 1960s. The bomb spike doubled the atmospheric ^{14}C level, an increase that was large enough to be easily measured as it moved into the upper ocean and finally toward the abyss. Like C_{ant}, the distribution of bomb-produced ^{14}C varies relative to a background of natural ^{14}C. Improved measurement technology has reduced sample-size requirements by a factor of 1,000 relative to the initial high-quality survey

(performed in the mid-1970s), and measurement precision has improved by a factor of two. Key et al. (2004) produced the first global three-dimensional maps of the distribution of measured, background, and bomb-produced ^{14}C, which were then integrated to yield inventories. The GO-SHIP sections from the 2000s have extended the time series, have been incorporated into GLODAPv2 (Olsen et al. 2014, 2015), and have allowed bomb-produced ^{14}C to be monitored as it is mixed into the ocean (**Figure 6**, **Supplemental Figures 7** and **8**).

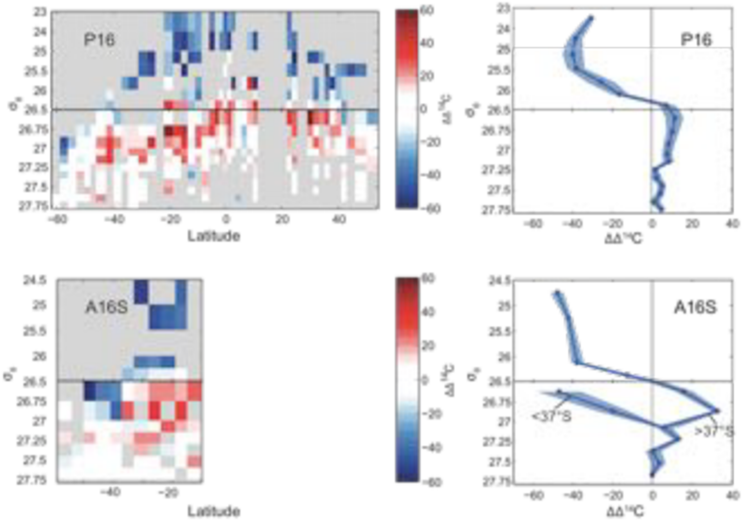

Figure 6 Changes in bomb-produced radiocarbon ($\Delta^{14}C$) on potential density σ_θ surfaces for two transects: (*a*) P16 in the Pacific along ~150°W (2005–2006 minus 1991) and (*b*) A16S in the South Atlantic along ~20°W (2005–2006 minus 1989). In the left subpanels, negative values (*blues* and *purples*) indicate a reduction in $\Delta^{14}C$, and positive values (*pinks* and *reds*) indicate an increase in $\Delta^{14}C$. The right panels show the zonally averaged differences as a function of potential density. Figure adapted from Graven et al. (2012).

Maps and inventories of ^{14}C have been used to determine global mean air-sea exchange rates for CO_2 (Naegler et al. 2006, Sweeney et al. 2007), calibrate global ocean general circulation models, and determine ocean ventilation rates (Matsumoto et al. 2004). More recently, Graven et al. (2012) have demonstrated that the temporal changes in ocean interior $\Delta^{14}C$ provide important independent constraints on the oceanic uptake of C_{ant}. This is because in recent decades, the oceanic uptake of ^{14}C (**Figure 6**) has been controlled largely by ocean circulation and mixing rather than by air-sea gas exchange, as was the case in the early decades after the bomb spike.

6. OCEAN VENTILATION: OXYGEN AND NUTRIENTS

6.1. Oxygen

Large and systematic changes in oxygen, mostly reductions, have been documented over the last two decades through GO-SHIP repeat hydrography and local station

time series (e.g., Keeling et al. 2010). The oxygen changes indicate large-scale changes in ventilation, temperature (as it impacts oxygen solubility), and possibly remineralization (which can impact ecosystem health) (Deutsch et al. 2015). Some of the observed oxygen changes could be due to changes in biology, but based on modeling studies (Deutsch et al. 2005) and correlations with physical forcing such as the North Atlantic Oscillation (Johnson & Gruber 2007), the consensus is that physical changes usually predominate. The combination of oxygen data with transient-tracer data provides further evidence regarding the timescales at which the ventilation changes occur (see Section 5.2). The combination of oxygen data with carbon data (e.g., Sabine et al. 2008) and pH data (e.g., Byrne et al. 2010) has allowed separation of DIC/pH changes along repeat sections into anthropogenic and ventilation/remineralization components, including their respective effects on carbon storage and ocean acidification.

The deoxygenation in the open-ocean thermocline over the past two decades is consistent with the expectation that warmer waters will hold less dissolved oxygen (the solubility effect) and that warming-induced stratification leads to a decrease in the transport of dissolved oxygen from surface to subsurface waters (the stratification effect) (Matear & Hirst 2003, Deutsch et al. 2005, Frölicher et al. 2009). Approximately 15% of the oxygen decline between 1970 and 1990 can be explained by warming and the remainder by increased stratification (Helm et al. 2011).

Oxygen decline is found most consistently in the oxygen minimum zones of the tropical Pacific, Atlantic, and Indian Oceans and in the subpolar and subtropical North Pacific and North Atlantic (Johnson & Gruber 2007; Keeling et al. 2010; Stramma et al. 2010, 2012; Keeling & Manning 2014). Differences between GO-SHIP and WOCE oxygen measurements on midocean meridional sections show these Northern Hemisphere declines as well as a decline within the Antarctic Circumpolar Current thermocline in the far south, as found by Aoki et al. (2005) (**Figure 5**).

Analyses in the North Atlantic over more than 50 years paint a more varied picture. Although the upper, mode, and intermediate waters are indeed losing oxygen because of changes in solubility, the deeper waters actually gained oxygen over this period owing to changes in circulation and ventilation (Stendardo & Gruber 2012). The trend in the North Pacific is based on a >50-year time series of oxygen data at ocean station P, which shows large bidecadal cycles on top of the smaller long-term trend (0.39–0.70 μmol kg^{-1} $year^{-1}$; Whitney et al. 2007), and on an ~30-year time series in the Oyashio off northern Japan, which also shows large bidecadal cycles on top of the long-term trend (0.9 ± 0.5 μmol kg^{-1} $year^{-1}$; Ono et al. 2001). The North Pacific GO-SHIP cruises have been instrumental in determining the spatial extent of the decadal-scale variations that extend into the subtropics in the east (e.g., Emerson et al. 2004, Mecking et al. 2008) and west (Kouketsu et al. 2010, Takatani et al. 2012, Sasano et al. 2015).

In contrast to the oxygen declines in many regions, oxygen in the subtropical Southern Hemisphere thermocline increased over the past few decades (**Figure 5** and **Supplemental Figure 9**). At 32°S in the Indian Ocean, McDonagh et al. (2005)

found a substantial increase in oxygen from 1987 to 2002, reversing an oxygen decline observed earlier (Bindoff & McDougall 2000). An oxygen increase also occurred over similar time periods along the 30°S repeat sections in the Pacific and Atlantic (Talley 2009). This oxygenation of the subtropical thermocline likely resulted from increased ventilation caused by spin-up of the Southern Hemisphere gyres (see Sections 3.2 and 5.1), documented at least for the Pacific based on dynamic height changes (Roemmich et al. 2007). The most recent 2009 repeat of the I5 section, however, indicates yet another reversal in gyre conditions, with oxygen decreasing (Mecking et al. 2012) (**Supplemental Figure 9**) in response to natural decadal variability as well as anthropogenic climate change (Kobayashi et al. 2012).

6.2. Nutrients

Nutrient-based geochemical studies have greatly increased understanding of basin-scale processes governing nutrients and oxygen. A linear combination of nitrate and phosphate, defined as N*, provides an estimate of excess nitrogen (e.g., from nitrogen fixation or atmospheric deposition) or nitrogen deficit (e.g., from denitrification or anammox) relative to global Redfield stoichiometry and is widely used for mapping the nitrogen cycle (**Supplemental Figure 10**). Use of N* has contributed to an upward revision of global estimates of nitrogen fixation (Moore & Doney 2007). Another geochemical tracer, Si*, representing the difference between silicic acid and nitrate concentrations, has shown the importance of Southern Ocean nutrient supply to the global thermocline north of 30°S (Sarmiento et al. 2004).

Nutrient changes observed over the past several decades have been attributed to (*a*) physical stratification and wind changes that also affect oxygen (see Section 6.1) and (*b*) human activities, mainly fossil fuel combustion and fertilizer production, that have increased atmospheric deposition and riverine discharge of nitrate to the ocean, thereby impacting the ocean biological carbon pump (Doney 2010). Over the past several decades, Whitney et al. (2013) have observed decreasing oxygen and increasing nutrients below the pycnocline in the subarctic Pacific, forced by changes in the advective flux of oxygen and nutrients, surface production and export, and remineralization. Interestingly, the vertical flux of nutrients to the euphotic zone remained relatively stable because increasing nutrient concentrations below the pycnocline offset an increase in pycnocline stratification. The long-term trends can be obscured by large interannual and multidecadal fluctuations in upper-ocean nutrient distributions that are coupled with climate modes of variability (Di Lorenzo et al. 2009, Henson et al. 2010).

In terms of human activities, Kim et al. (2014) used N* measurements and CFC-based ventilation rates to determine that atmospheric deposition of anthropogenic nitrate in the western North Pacific has been associated with increasing excess nitrate in the upper water column over the last 30 years. The effect was highest close to Asia, a source regions for reactive nitrate, with rates decreasing eastward across the North Pacific. This input may eventually transform this ecosystem from nitrate to phosphate limitation (Kim et al. 2014). In the North Atlantic subtropical gyre, rates of atmospheric nitrate deposition are comparable to estimated rates of N_2 fixation, but reactive nitrate is rapidly consumed and does not accumulate in surface

waters (Zamora et al. 2010). Instead, excess nitrate is accumulating in the main thermocline, with ~15–20% attributable to atmospheric deposition (Hansell et al. 2007, Zamora et al. 2010).

Detection of long-term climate trends in the presence of natural variability and current nutrient data uncertainty will require many decades of sustained observation and improved measurement accuracy during GO-SHIP cruises. Utilization of historical nutrient data to access decadal trends in the oceans has been hindered by their inaccuracy, manifested as offsets in deep water concentrations measured by different laboratories (Zhang et al. 2000). At present, development of Certified Reference Materials for seawater nutrient measurement is underway and their widespread use in shipboard measurements in conjunction with unified methodology and instrumentation will improve the internal consistency of the global nutrient dataset generated in GO-SHIP (National Research Council 2002).

SUMMARY POINTS

1. The ocean is warming, taking up the majority of the excess heat in the Earth system over recent decades; approximately 19% of this heat is below 2,000 m.
2. Abyssal waters originating in the Southern Ocean have been warming; those from the Pacific and Indian sectors have also been freshening.
3. In many regions, vertical diffusivity increases from a minimum in the thermocline to a maximum within the bottom 1,500 m.
4. Increased stratification has resulted in a decline in oxygen and increase in nutrients in the Northern Hemisphere thermocline and an expansion of the tropical oxygen minimum zones. Southern Hemisphere thermocline oxygen increased in the 2000s owing to stronger wind forcing that increased the ventilation of the subtropical gyres, supported by evidence from transient tracer changes.
5. Anthropogenic carbon uptake has been quantified and mapped, with supporting evidence from transient tracers including chlorofluorocarbons (CFCs) and radiocarbon; the oceans currently sequester approximately 27% of the anthropogenic carbon released to the atmosphere by fossil fuel burning and land-use change.
6. As anthropogenic CO_2 invades the ocean, the upper ocean is acidifying.
7. Dissolved organic carbon, a large, bioactive reservoir, has been mapped and inventoried for the first time, and its contribution to export production (~20%) and deep-ocean oxygen utilization have been quantified.
8. Atmospheric and riverine inputs of anthropogenic nutrients have changed the ocean biogeochemistry in the upper waters of the western North Pacific and the thermocline of the North Atlantic.

FUTURE ISSUES

1. Sustaining the ship-based, full-depth ocean observations coordinated through GO-SHIP is of high priority, particularly because we anticipate accelerating changes in the coming decades.
2. GO-SHIP evolves with experience and with new technology. We look forward to incorporating advances in biological and biogeochemical sensing techniques that will expand the role of GO-SHIP in documenting long-term changes in marine biogeochemistry and ecosystems.

DISCLOSURE STATEMENT

B.M.S. and R.W. are co-chairs and M.K. is project coordinator of the international GO-SHIP program. L.D.T., R.A.F. and G.C.J. are co-chairs of the U.S. GO-SHIP program. C.A.C. is co-editor and R.A.F. is a member of the editorial committee of Annual Reviews of Marine Science. All authors have received funding related to the program results reported in this review.

ACKNOWLEDGMENTS

We acknowledge support from the Climate Observations Division of the US National Oceanic and Atmospheric Administration (NOAA) Climate Program Office and NOAA Research; the Joint Institute for the Study of the Atmosphere and Ocean (JISAO) under NOAA cooperative agreement NA10OAR4320148; NOAA grant NA11OAR4310063; the US National Science Foundation (grants OCE-0223869, OCE-0752970, OCE-0825163, OCE-1434000, OCE-0752972, OCE-0752980, OCE-1232962, OCE-1155983, and OCE-1436748); the US CLIVAR Project Office; the Global Environment and Marine Department of the Japan Meteorological Agency; the Australian Climate Change Science Program of the Australian Department of Environment and Commonwealth Scientific and Industrial Research Organisation (CSIRO); the UK Natural Environment Research Council; the European Union (FP7 grant agreement 264879, CarboChange); Horizon 2020 (grant agreement 633211); and ETH Zurich. This is JISAO contribution number 2434 and NOAA Pacific Marine Environmental Laboratory contribution number 4329. Affiliations for the authors of this article are as follows:

[1]Scripps Institution of Oceanography, University of California, San Diego, La Jolla, California 92093; email: ltalley@ucsd.edu, jswift@ucsd.edu

[2]Pacific Marine Environmental Laboratory, National Oceanic and Atmospheric Administration, Seattle, Washington 98115; email: richard.a.feely@noaa.gov, john.l.bullister@noaa.gov, gregory.c.johnson@noaa.gov, jeremy.mathis@noaa.gov, chris.sabine@noaa.gov

[3]Commonwealth Scientific and Industrial Research Organisation (CSIRO), Hobart, Tasmania 7001, Australia; email: bernadette.sloyan@csiro.au

[4]Atlantic Oceanographic and Meteorological Laboratory, National Oceanic and Atmospheric Administration, Miami, Florida 33149; email: rik.wanninkhof@noaa.gov, molly.baringer@noaa.gov, jia-zhong.zhang@noaa.gov

[5]Department of Ecology, Evolution, and Marine Biology, University of California, Santa Barbara, Santa Barbara, California 93106; email: carlson@lifesci.ucsb.edu
[6]Woods Hole Oceanographic Institution, Woods Hole, Massachusetts 02543; email: sdoney@whoi.edu, amacdonald@whoi.edu
[7]Rosenstiel School of Marine and Atmospheric Science, University of Miami, Miami, Florida 33149; email: rfine@rsmas.miami.edu, dhansell@rsmas.miami.edu, clangdon@rsmas.miami.edu, fmillero@rsmas.miami.edu
[8]Department of Oceanography, University of Hawai'i at Mānoa, Honolulu, Hawaii 96822; email: efiring@hawaii.edu
[9]Institute of Biogeochemistry and Pollutant Dynamics, ETH Zurich, Zurich 8092, Switzerland; email: nicolas.gruber@env.ethz.ch
[10]Meteorological Research Institute, Japan Meteorological Agency, Tsukuba 305-0052, Japan; email: mishii@mri-jma.go.jp
[11]Japan Agency for Marine-Earth Science and Technology (JAMSTEC), Yokosuka 237-0061, Japan; email: k.katsumata@jamstec.go.jp
[12]Program in Atmospheric and Oceanic Sciences, Princeton University, Princeton, New Jersey 08544; email: key@princeton.edu
[13]JCOMM in-situ Observations Programme Support Center (JCOMMOPS), Technopôle Brest Iroise, Plouzané 29280, France; email: mkramp@jcommops.org
[14]National Oceanography Centre, Southampton SO14 3ZH, United Kingdom; email: e.mcdonagh@noc.ac.uk
[15]Applied Physics Laboratory, University of Washington, Seattle, Washington 98105; email: mecking@uw.edu
[16]Joint Institute for the Study of the Atmosphere and Ocean, University of Washington, Seattle, Washington 98195; email: mordy@uw.edu
[17]Japan Meteorological Agency, Tokyo 100-8122, Japan; email: nakano_t@met.kishou.go.jp
[18]Lamont-Doherty Earth Observatory, Columbia University, Palisades, New York 10964; email: bsmeth@ldeo.columbia.edu, ant@ldeo.columbia.edu
[19]GEOMAR Helmholtz Centre for Ocean Research Kiel, 24015 Kiel, Germany; email: ttanhua@geomar.de
[20]School of Oceanography, University of Washington, Seattle, Washington 98195; email: warner@u.washington.edu

LITERATURE CITED

Antonov JI, Locarnini RA, Boyer TP, Mishonov AV, and Garcia HE. 2006. *World Ocean Atlas 2005, Volume 2: Salinity*, ed. S Levitus, NOAA Atlas NESDIS 62, U.S. Government Printing Office, Washington, D.C., 182 pp

Aoki S, Bindoff NL, Church JA. 2005. Interdecadal water mass changes in the Southern Ocean between 30°E and 160°E. *Geophys. Res. Lett.* 32:L07607

Arístegui J, Duarte CM, Agustí S, Doval M, Álvarez-Salgado XA, Hansell DA. 2002. Dissolved organic carbon support of respiration in the dark ocean. *Science* 298: 1967

Bindoff NL, McDougall TJ. 2000. Decadal changes along an Indian Ocean section at 32°S and their interpretation. *J. Phys. Oceanogr.* 30:1207–22

Bindoff NL, Willebrand J, Artale V, Cazenave A, Gregory J, et al. 2007. Observations: oceanic climate change and sea level. In *Climate Change 2007: The Physical Science Basis. Contribution of Working Group I to the Fourth Assessment Report of the Intergovernmental Panel on Climate Change*, ed. S Solomon, D Qin, M Manning, Z Chen, M Marquis, et al., pp. 385–432. Cambridge, UK: Cambridge Univ. Press

Boyer TP, Levitus S, Antonov JI, Locarnini RA, Garcia HE. 2005. Linear trends in salinity for the World Ocean, 1955–1998. *Geophys. Res. Lett.* 32:L01604

Brown PJ, Bakker DCE, Schuster U, Watson AJ. 2010. Anthropogenic carbon accumulation in the subtropical North Atlantic. *J. Geophys. Res.* 115:C04016

Bryden HL, Longworth HR, Cunningham SA. 2005. Slowing of the Atlantic meridional overturning circulation at 25°N. *Nature* 438:655–57

Bryden HL, McDonagh EL, King BA. 2003. Changes in ocean water mass properties: oscillations or trends? *Science* 27:2086–88

Bullister JL. 2015. *Atmospheric histories (1765–2015) for CFC-11, CFC-12, CFC-113, CCl_4, SF_6 and N_2O.* ORNL/CDIAC-161, NDP-095. Carbon Dioxide Inf. Anal. Cent., Oak Ridge Natl. Lab., Oak Ridge, TN. Data product at ORNL, http://cdiac.ornl.gov/oceans/CFC_ATM_Hist2015.html, doi:10.3334/CDIAC/otg.CFC_ATM_Hist_2015.

Bullister JL, Wisegarver DP, Menzia FA. 2002. The solubility of sulfur hexafluoride in water and seawater. *Deep-Sea Res. I* 49:175–87

Byrne RH, Mecking S, Feely RA, Liu X. 2010. Direct observations of basin-wide acidification of the North Pacific. *Geophys. Res. Lett.* 37:L02601

Carlson CA, Ducklow HW, Michaels AF. 1994. Annual flux of dissolved organic carbon from the euphotic zone in the northwestern Sargasso Sea. *Nature* 371:405–8

Carlson CA, Hansell DA. 2015. DOM sources, sinks, reactivity and budgets. In *Biogeochemistry of Marine Dissolved Organic Matter*, ed. DA Hansell, CA Carlson, pp. 65–126. New York: Academic. 2nd ed.

Carlson CA, Hansell DA, Nelson NB, Siegel DA, Smethie WM, et al. 2010. Dissolved organic carbon export and subsequent remineralization in the mesopelagic and bathypelagic realms of the North Atlantic basin. *Deep-Sea Res. II* 57:1433–45

Carton JA, Cunningham SA, Frajka-Williams E, Kwon Y-O, Marshall DP, Msadek R. 2014. The Atlantic overturning circulation: more evidence of variability and links to climate. *Bull. Amer. Meteor. Soc.* 95:ES163–66

Carton JA, Hakkinen S. 2011. Introduction to: Atlantic Meridional Overturning Circulation (AMOC). *Deep-Sea Res. II* 58:1741–43

Church JA, White NJ, Konikow LF, Domingues CM, Cogley JG, et al. 2011. Revisiting the Earth's sea level and energy budgets from 1961 to 2008. *Geophys. Res. Lett.* 38:L18601

Copin-Montgut G, Avril B. 1993. Vertical distribution and temporal variation of dissolved organic carbon in the North-Western Mediterranean Sea. *Deep-Sea Res. I* 40:1963–72

Curry RG, McCartney MS. 2001. Ocean gyre circulation changes associated with the North Atlantic Oscillation. *J. Phys. Oceanogr.* 31:3374–400

Decloedt T, Luther DS. 2012. Spatially heterogeneous diapycnal mixing in the abyssal ocean: a comparison of two parameterizations to observations. *J. Geophys. Res.* 117:C11025

Deutsch C, Emerson S, Thompson L. 2005. Fingerprints of climate change in North Pacific oxygen. *Geophys. Res. Lett.* 32:L16604

Di Lorenzo E, Fiechter J, Schneider N, Bracco A, Miller AJ, et al. 2009. Nutrient and salinity decadal variations in the central and eastern North Pacific. *Geophys. Res. Lett.* 36:L14601

Doney SC. 2010. The growing human footprint on coastal and open-ocean biogeochemistry. *Science* 328:1512–16

Doney SC, Jenkins WJ. 1994. Ventilation of the deep western boundary current and the abyssal western North Atlantic: estimates from tritium and ^{3}He distributions. *J. Phys. Oceanogr.* 24:638–59

Doney SC, Jenkins WJ, Bullister JL. 1997. A comparison of ocean tracer dating techniques on a meridional section in the eastern North Atlantic. *Deep-Sea Res. I* 44:603–26

Durack PJ, Wijffels SE. 2010. Fifty-year trends in global ocean salinities and their relationship to broad-scale warming. *J. Clim.* 23:4342–62

Durack PJ, Wijffels SE, Matear RJ. 2012. Ocean salinities reveal strong global water cycle intensification during 1950 to 2000. *Science* 336:455–58

Dutay J-C, Bullister JL, Doney SC, Orr JC, Najjar R, et al. 2002. Evaluation of ocean model ventilation with CFC-11: comparison of 13 global ocean models. *Ocean Model.* 4:89–120

Egleston ES, Sabine CL, Morel FMM. 2010. Revelle revisited: Buffer factors that quantify the response of ocean chemistry to changes in DIC and alkalinity. *Global Biogeochem. Cycles* 24, GB1002, doi:.1029/2008GB003407

Emerson S, Mecking S, Abell J. 2001. The biological pump in the subtropical North Pacific Ocean: nutrient sources, Redfield ratios, and recent changes. *Glob. Biogeochem. Cycles* 15:535–54

Emerson S, Watanabe YW, Ono T, Mecking S. 2004. Temporal trends in apparent oxygen utilization in the upper pycnocline of the North Pacific: 1980–2000. *J. Oceanogr.* 60:139–47

Feely RA, Doney SC, Cooley SR. 2009. Ocean acidification: present conditions and future changes in a high-CO_2 world. *Oceanography* 22(4):36–47

Feely RA, Sabine CL, Lee K, Berelson W, Kleypas J, et al. 2004. Impact of anthropogenic CO_2 on the $CaCO_3$ system in the oceans. *Science* 305:362–66

Fine RA. 2011. Observations of CFCs and SF_6 as ocean tracers. *Annu. Rev. Mar. Sci.* 3:173–95

Fine RA, Peacock S, Maltrud ME, Bryan FO. 2014. *A new look at ocean ventilation timescales*. Presented at Ocean Sci. Meet., Honolulu, HI, Feb. 23–28. http://www.sgmeet.com/osm2014/viewabstract.asp?abstractid=14982

Frajka-Williams E, Cunningham SA, Bryden H, King BA. 2011. Variability of Antarctic Bottom Water at 24.5°N in the Atlantic. *J. Geophys. Res.* 116:C11026

Friis K, Körtzinger A, Pätsch J, Wallace DWR. 2005. On the temporal increase of anthropogenic CO_2 in the subpolar North Atlantic. *Deep-Sea Res. I* 52:681–98

Frölicher TL, Joos F, Plattner GK, Steinacher M, Doney SC. 2009. Natural variability and anthropogenic trends in oceanic oxygen in a coupled carbon cycle-climate model ensemble. *Glob. Biogeochem. Cycles* 23:GB1003

Frölicher TL, Winton M, Sarmiento JL. 2014. Continued global warming after CO_2 emissions stoppage. *Nat. Clim. Change* 4:40–44

Fukasawa M, Freeland H, Perkin R, Watanabe T, Uchida H, Nishina A. 2004. Bottom water warming in the North Pacific Ocean. *Nature* 427:825–27

Ganachaud A, Wunsch C. 2000. Improved estimates of global ocean circulation, heat transport and mixing from hydrographic data. *Nature* 408:453–56

Gloor M, Gruber N, Sarmiento JL, Sabine CL, Feely RA, Rödenbeck C. 2003. A first estimate of present and preindustrial air-sea CO_2 flux patterns based on ocean interior carbon measurements and models. *Geophys. Res. Lett.* 30:1010

Goldberg S, Carlson C, Brzezinski M, Nelson N, Siegel D. 2011. Systematic removal of neutral sugars within dissolved organic matter across ocean basins. *Geophys. Res. Lett.* 38:L17606

Graven HD, Gruber N, Key R, Khatiwala S, Giraud X. 2012. Changing controls on oceanic radiocarbon: new insights on shallow-to-deep ocean exchange and anthropogenic CO_2 uptake. *J. Geophys. Res.* 117:C10005

Gregg MC. 1989. Scaling turbulent dissipation in the thermocline. *J. Geophys. Res.* 94:9686–98

Gregg MC, Sanford TB, Winkel DP. 2003. Reduced mixing from the breaking of internal waves in equatorial waters. *Nature* 422:513–15

Gruber N, Gloor M, Mikaloff Fletcher SE, Doney SC, Dutkiewicz S, et al. 2009. Oceanic sources, sinks, and transport of atmospheric CO_2. *Glob. Biogeochem. Cycles* 23:GB1005

Gruber N, Sarmiento JL, Stocker TF. 1996. An improved method for detecting anthropogenic CO_2 in the oceans. *Glob. Biogeochem. Cycles* 10:809–37

Hakkinen S, Hatun H, Rhines PB. 2008. Satellite evidence of change in the northern gyre. In *Arctic-Subarctic Ocean Fluxes: Defining the Role of the Northern Seas in Climate*, ed. B Dickson, J Meincke, P Rhines, pp. 551–67. Dordrecht, Neth.: Springer

Hakkinen S, Rhines PB. 2004. Decline of subpolar North Atlantic circulation during the 1990s. *Science* 302:555–59

Hall TM, Haine TWN, Holzer M, LeBel DA, Terenzi F, Waugh DW. 2007. Ventilation rates estimated from tracers in the presence of mixing. *J. Phys. Oceanogr.* 37:2599–611

Hansell DA. 2013. Recalcitrant dissolved organic carbon fractions. *Annu. Rev. Mar. Sci.* 5:421–45

Hansell DA, Carlson CA, Repeta DJ, Schlitzer R. 2009. Dissolved organic matter in the ocean: A controversy stimulates new insights. *Oceanography* 22(4):202–11, http://dx.doi.org/10.5670/oceanog.2009.109

Hansell DA, Carlson CA, Schlitzer R. 2012. Net removal of major marine dissolved organic carbon fractions in the subsurface ocean. *Glob. Biogeochem. Cycles* 26:GB1016

Hansell DA, Olson DB, Dentener F, Zamora LM. 2007. Assessment of excess nitrate development in the subtropical North Atlantic. *Mar. Chem.* 106:562–79

Hartin CA, Fine RA, Kamenkovich I, Sloyan BM. 2014. Comparison of Subantarctic Mode Water and Antarctic Intermediate Water formation rates in the South Pacific between NCAR-CCSM4 and observations. *Geophys. Res. Lett.* 41:519–26
Helm KP, Bindoff NL, Church JA. 2010. Changes in the global hydrological-cycle inferred from ocean salinity. *Geophys. Res. Lett.* 37:L18701
Helm KP, Bindoff NL, Church JA. 2011. Observed decreases in oxygen content of the global ocean. *Geophys. Res. Lett.* 38:L23602
Henson SA, Sarmiento JL, Dunne JP, Bopp L, Lima I, et al. 2010. Detection of anthropogenic climate change in satellite records of ocean chlorophyll and productivity. *Biogeosciences* 7: 621-640
Henyey FS, Wright JA, Flatté SM. 1986. Energy and action flow through the internal wave field: an eikonal approach. *J. Geophys. Res.* 91:8487–95
Hernández-Guerra A, Pelegri JL, Fraile-Nuez E, Benitez-Barrios V, Emilianov M, et al. 2014. Meridional overturning transports at 7.5N and 24.5N in the Atlantic Ocean during 1992–93 and 2010–11. *Prog. Oceanogr.* 128:98–114
Holzer M, Primeau FW, Smethie WM, Khatiwala S, Hall T. 2010. Where and how long ago was water in the western North Atlantic ventilated? Maximum-entropy inversions of bottle data from WOCE line A20. *J. Geophys. Res.* 115:C07005
Huhn O, Rhein M, Hoppema M, van Heuven S. 2013. Decline of deep and bottom water ventilation and slowing down of anthropogenic carbon storage in the Weddell Sea, 1984–2011. *Deep-Sea Res. I* 76:66–84
Huussen TN, Naveira-Garabato AC, Bryden HL, McDonagh EL. 2012. Is the deep Indian Ocean MOC sustained by breaking internal waves? *J. Geophys. Res.* 117:C08024
Jacobs SS, Giulivi CF. 2010. Large multidecadal salinity trends near the Pacific Antarctic continental margin. *J. Clim.* 23:4508–24
Jenkins WJ. 1977. Tritium-helium dating in the Sargasso Sea: a measurement of oxygen utilization rates. *Science* 196:291–92
Jenkins WJ. 1998. Studying thermocline ventilation and circulation using tritium and ^{3}He. *J. Geophys. Res.* 103:15817–31
Johnson GC. 2008. Quantifying Antarctic Bottom Water and North Atlantic Deep Water volumes. *J. Geophys. Res.* 113:C05027
Johnson GC, Gruber N. 2007. Decadal water mass variations along 20°W in the northeastern Atlantic Ocean. *Prog. Oceanogr.* 73:277–95
Johnson GC, McTaggart KE, Wanninkhof R. 2014. Antarctic Bottom Water temperature changes in the western South Atlantic from 1989 to 2014. *J. Geophys. Res.* 119:8567–77
Johnson GC, Purkey SG, Toole JM. 2008. Reduced Antarctic meridional overturning circulation reaches the North Atlantic Ocean. *Geophys. Res. Lett.* 35:L22601
Katsumata K, Masuda S. 2013. Variability in Southern Hemisphere ocean circulation from the 1980s to the 2000s. *J. Phys. Oceanogr.* 43:1981–2007
Katsumata K, Nakano H, Kumamoto Y. 2015. Dissolved oxygen change and freshening of Antarctic Bottom water along 62°S in the Australian-Antarctic Basin between 1995/1996 and 2012/2013. *Deep-Sea Res. II* 114:27–38
Keeling RF, Körtzinger A, Gruber N. 2010. Ocean deoxygenation in a warming world. *Annu. Rev. Mar. Sci.* 2:199–229

Keeling RF, Manning AC. 2014. Studies of recent changes in atmospheric O_2 content. In *Treatise on Geochemistry*, Vol. 5: *The Atmosphere*, ed. HD Holland, KK Turekian, pp. 385–404. Amsterdam: Elsevier. 2nd ed.
Key RM, Kozyr A, Sabine CL, Lee K, Wanninkhof R, et al. 2004. A global ocean carbon climatology: results from Global Data Analysis Project (GLODAP). *Glob. Biogeochem. Cycles* 19:GB4031
Khatiwala S, Primeau F, Hall T. 2009. Reconstruction of the history of anthropogenic CO_2 concentrations in the ocean. *Nature* 462:346–49
Khatiwala S, Tanhua T, Mikaloff Fletcher S, Gerber M, Doney SC, et al. 2013. Global ocean storage of anthropogenic carbon. *Biogeosciences* 10:2169–91
Kieke D, Rhein M, Stramma L, Smethie WM, Bullister JL, LeBel DA. 2007. Changes in the pool of Labrador Sea Water in the subpolar North Atlantic. *Geophys. Res. Lett.* 34:L06605
Kieke D, Rhein M, Stramma L, Smethie WM, LeBel DA, Zenk W. 2006. Changes in the CFC inventories and formation rates of Upper Labrador Sea Water, 1997–2001. *J. Phys. Oceanogr.* 36:64–86
Kim IN, Lee K, Gruber N, Karl DM, Bullister JL, et al. 2014. Increasing anthropogenic nitrogen in the North Pacific Ocean. *Science* 346:1102–6
Kobayashi T, Mizuno K, Suga T. 2012. Long-term variations of surface and intermediate waters in the southern Indian Ocean along 32°S. *J. Oceanogr.* 68:243–65
Körtzinger A, Rhein M, Mintrop L. 1999. Anthropogenic CO_2 and CFCs in the North Atlantic Ocean—a comparison of man-made tracers. *Geophys. Res. Let.* 26:2065–68
Kouketsu S, Doi T, Kawano T, Masuda S, Sugiura N, et al. 2011. Deep ocean heat content changes estimated from observation and reanalysis product and their influence on sea level change. *J. Geophys. Res.* 116:C03012
Kouketsu S, Fukasawa M, Kaneko I, Kawano T, Uchida H, et al. 2009. Changes in water properties and transports along 24°N in the North Pacific between 1985 and 2005. *J. Geophys. Res.* 114:C01008
Kouketsu S, Fukasawa M, Sasano D, Kumamoto Y, Kawano T, et al. 2010. Changes in water properties around North Pacific intermediate water between the 1980s, 1990s and 2000s. *Deep-Sea Res. II* 57:1177–87
Kouketsu S, Murata AM. 2014. Detecting decadal scale increases in anthropogenic CO_2 in the ocean. *Geophys. Res. Lett.* 41:4594–600
Kunze E, Firing E, Hummon JM, Chereskin TK, Thurnherr AM. 2006. Global abyssal mixing from lowered ADCP shear and CTD strain profiles. *J. Phys. Oceanogr.* 36:1553–76
LaCasce JH, Ferrari R, Marshall J, Tulloch R, Balwada D, Speer K. 2014. Float-derived isopycnal diffusivities in the DIMES experiment. *J. Phys. Oceanogr.* 44:764–80
Landschützer P, Gruber N, Bakker DCE, Schuster U. 2014. Recent variability of the global ocean carbon sink. *Glob. Biogeochem. Cycles* 28:927–49
LeBel DA, Smethie WM, Rhein M, Kieke D, Fine RA, et al. 2008. The formation rate of North Atlantic Deep Water and Eighteen Degree Water calculated from CFC-11 inventories observed during WOCE. *Deep-Sea Res. I* 55:891–910

Levine NM, Doney SC, Lima I, Wanninkhof R, Bates NR, Feely RA. 2011. The impact of the North Atlantic Oscillation on the uptake and accumulation of anthropogenic CO_2 by North Atlantic Ocean mode waters. *Glob. Biogeochem. Cycles* 25:GB3022

Levine NM, Doney SC, Wanninkhof R, Lindsay K, Fung I. 2008. Impact of ocean carbon system variability on the detection of temporal increases in anthropogenic CO_2. *J. Geophys. Res.* 113:C03019

Locarnini RA, Mishonov AV, Antonov JI, Boyer TP, and Garcia HE. 2006. *World Ocean Atlas 2005, Volume 1: Temperature*. S Levitus, Ed. NOAA Atlas NESDIS 61, U.S. Government Printing Office, Washington, D.C., 182 pp.

Locarnini RA, Mishonov AV, Antonov JI, Boyer TP, Garcia HE, et al. 2013. *World Ocean Atlas 2013, Volume 1: Temperature.* S Levitus, Ed., A Mishonov Technical Ed.; NOAA Atlas NESDIS 73, 40 pp.

Loeb NG, Lyman JM, Johnson GC, Doelling DR, Wong T, et al. 2012. Observed changes in top-of-the-atmosphere radiation and upper-ocean heating consistent within uncertainty. *Nat. Geosci.* 5:110–13

Long MC, Lindsay K, Peacock S, Moore JK, Doney SC. 2013. Twentieth-century ocean carbon uptake and storage in CESM1(BGC). *J. Clim.* 26:6775–800

Longworth HR, Bryden HL, Baringer MO. 2011. Historical variability in Atlantic meridional baroclinic transport at 26.5°N from boundary dynamic height observations. *Deep-Sea Res. II* 58:1754–67

Lozier MS. 2010. Deconstructing the conveyor belt. *Science* 328:1507–11

Lumpkin R, Speer K. 2007. Global ocean meridional overturning. *J. Phys. Oceanogr.* 37:2550–62

Macdonald AM, Mecking S, Robbins PE, Toole JM, Johnson GC, et al. 2009. The WOCE-Era 3-D Pacific Ocean circulation and heat budget. *Prog. Oceanogr.* 82:281–325

Masuda S, Awaji T, Sugiura N, Matthews JP, Toyoda T, et al. 2010. Simulated rapid warming of abyssal North Pacific water. *Science* 329:319–22

Matear RJ, Hirst AC. 2003. Long-term changes in dissolved oxygen concentrations in the ocean caused by protracted global warming. *Glob. Biogeochem. Cycles* 17:1125

Matsumoto K, Sarmiento JL, Key RM, Bullister JL, Caldeira K, et al. 2004. Evaluation of ocean carbon cycle models with data-based metrics. *Geophys. Res. Lett.* 31:L07303

Mauritzen C, Melsom A, Sutton RT. 2012. Importance of density-compensated temperature change for deep North Atlantic Ocean heat uptake. *Nat. Geosci.* 5:905–10

McCarthy G, Smeed DA, Johns WE, Frajka-Williams E, Moat BI, et al. 2015. Measuring the Atlantic meridional overturning circulation at 26°N. *Prog. Oceanogr.* 130:91–111

McDonagh EL, Bryden HL, King BA, Sanders RJ. 2008. The circulation of the Indian Ocean at 32°S. *Prog. Oceanogr.* 79:20–36

McDonagh EL, Bryden HL, King BA, Sanders RJ, Cunningham SA, Marsh R. 2005. Decadal changes in the South Indian Ocean thermocline. *J. Clim.* 18:1575–90

Mecking S, Johnson GC, Bullister JL, Macdonald AM. 2012. *Decadal changes in oxygen and temperature-salinity relations along 32°S in the Indian Ocean through 2009*.

Presented at Ocean Sci. Meet., Salt Lake City, UT, Feb. 20–24. https://www.sgmeet.com/osm2012/viewabstract2.asp?AbstractID=10467
Mecking S, Langdon C, Feely RA, Sabine CL, Deutsch CA, Min D-H. 2008. Climate variability in the North Pacific thermocline diagnosed from oxygen measurements: an update based on the US CLIVAR/CO_2 Repeat Hydrography cruises. *Glob. Biogeochem. Cycles* 22:GB3015
Mecking S, Warner MJ, Bullister JL. 2006. Temporal changes in pCFC-12 ages and AOU along two hydrographic sections in the eastern subtropical North Pacific. *Deep-Sea Res. I* 53:169–87
Melet A, Hallberg R, Legg S, Polzin KL. 2013. Sensitivity of the Pacific Ocean state to the vertical distribution of internal-tide driven mixing. *J. Phys. Oceanogr.* 43:602–15
Moore, JK, Doney SC. 2007. Iron availability limits the ocean nitrogen inventory stabilizing feedbacks between marine denitrification and nitrogen fixation. *Global Biogeochem. Cycles* 21:GB2001. doi:10.1029/2006GB002762
Munk W. 1966. Abyssal recipes. *Deep-Sea Res.* 13:707–30
Murata A, Kumamoto Y, Sasaki K, Watanabe S, Fukasawa M. 2008. Decadal increases of anthropogenic CO in the subtropical South Atlantic Ocean along 30°S. *J. Geophys. Res.* 113:C06007
Murata A, Kumamoto Y, Sasaki K, Watanabe S, Fukasawa M. 2010. Decadal increases in anthropogenic CO_2 along 20°S in the South Indian Ocean. *J. Geophys. Res.* 115:C12055
Murata A, Kumamoto Y, Watanabe S, Fukasawa M. 2007. Decadal increases of anthropogenic CO_2 in the South Pacific subtropical ocean along 32°S. *J. Geophys. Res.* 112:C05033
Naegler T, Ciais P, Rodgers KB, Levin I. 2006. Excess radiocarbon constraints on air-sea gas exchange and the uptake of CO_2 by the oceans. *Geophys. Res. Lett.* 33:L11802
Nakano T, Kitamura T, Sugimoto S, Suga T, Kamachi M. 2015. Long-term variations of North Pacific Tropical Water along the 137°E repeat hydrographic section. *J. Oceanogr.* 71:229–38
National Research Council, Committee on Reference Materials for Ocean Science. 2002. Chemical reference materials: setting the standards for ocean science. *The National Academies Press*, Washington DC, 144 pp.
Naveira Garabato AC, Polzin KL, King BA, Heywood KJ, Visbeck M. 2004. Widespread intense turbulent mixing in the Southern Ocean. *Science* 303:210–13
Olsen A, Key RM, Lauvset SK, Lin X, Tanhua T, et al. 2014. *Release! Global Ocean Data Analysis Version 2 (GLODAPv.2)*. Presented at Ocean Sci. Meet., Honolulu, HI, Feb. 23–28. http://www.sgmeet.com/osm2014/viewabstract.asp?abstractid=15764
Olsen A, Key RM, Lauvset SK, Van Heuven S, Lin X, et al. 2015. GLODAPv.2, GLobal Ocean Data Analysis Project Version 2, CDIAC, NDP (to be submitted)
Ono T, Midorikawa T, Watanabe Y, Tadokoro K, Saino T. 2001. Temporal increases of phosphate and apparent oxygen utilization in the subsurface waters of western subarctic Pacific from 1968 to 1998. *Geophys. Res. Lett.* 28:3285–88
Orr JC, Fabry VJ, Aumont O, Bopp L, Doney SC, et al. 2005. Anthropogenic ocean acidification over the twenty-first century and its impact on calcifying organisms. *Nature* 437:681–86

Orsi AH, Smethie WM, Bullister JL. 2002. On the total input of Antarctic waters to the deep ocean: a preliminary estimate from chlorofluorocarbon measurements. *J. Geophys. Res.* 107:31-1–14
Orsi AH, Whitworth T, Nowlin WD. 1995. On the meridional extent and fronts of the Antarctic Circumpolar Current. *Deep-Sea Res. I.* 42: 641-673
Palmer MD, Bryden HL, Hirschi J, Marotzke J. 2004. Observed changes in the South Indian Ocean gyre circulation, 1987–2002. *Geophys. Res. Lett.* 31:L15303
Pardo PC, Pérez FF, Khatiwala S, Ríos AF. 2014. Anthropogenic CO_2 estimates in the Southern Ocean: Storage partitioning in the different water masses. *Prog. Oceanogr.* 120:230–42
Peacock S, Maltrud M, Bleck R. 2005. Putting models to the data test: a case study using Indian Ocean CFC-11 data. *Ocean Model.* 9:1–22
Pérez FF, Mercier H, Vázquez-Rodríguez M, Lherminier P, Velo A, et al. 2013. Atlantic Ocean CO_2 uptake reduced by weakening of the meridional overturning circulation. *Nat. Geosci.* 6:146–52, 10.1038/ngeo1680
Pérez FF, Vázquez-Rodríguez M, Mercier H, Velo A, Lherminier P, Ríos AF. 2010. Trends of anthropogenic CO_2 storage in North Atlantic water masses. *Biogeosciences* 7:1789–807
Polzin KL, Garabato ACN, Huussen TN, Sloyan BM, Waterman S. 2014. Finescale parameterizations of turbulent dissipation. *J. Geophys. Res. Oceans* 119:1383–419
Polzin KL, Toole JM, Schmitt RW. 1995. Finescale parameterizations of turbulent dissipation. *J. Phys. Oceanogr.* 25:306–28
Purkey SG, Johnson GC. 2010. Warming of global abyssal and deep Southern Ocean waters between the 1990s and 2000s: contributions to global heat and sea level rise budgets. *J. Clim.* 23:6336–51
Purkey SG, Johnson GC. 2012. Global contraction of Antarctic Bottom Water between the 1980s and 2000s. *J. Clim.* 25:5830–44
Purkey SG, Johnson GC. 2013. Antarctic Bottom Water warming and freshening: contributions to sea level rise, ocean freshwater budgets, and global heat gain. *J. Clim.* 26:6105–22
Rahmstorf S, Box JE, Feulner G, Mann ME, Robinson A, et al. 2015. Exceptional twentieth-century slowdown in Atlantic Ocean overturning circulation. *Nat. Clim. Change* 5:475–80
Rayner D, Hirschi JMM, Kanzow T, Johns WE, Wright PG, et al. 2011. Monitoring the Atlantic meridional overturning circulation. *Deep-Sea Res. II* 58:1744–53
Rhein M, Fischer J, Smethie WM, Smythe-Wright D, Min DH, et al. 2002. Labrador Sea Water: pathways, CFC inventory and formation rates. *J. Phys. Oceanogr.* 32:648–65
Rhein M, Kieke DH, Huttl-Kabus S, Roessler A, Mertens C, et al. 2011. Deep water formation, the subpolar gyre, and the meridional overturning circulation in the subpolar North Atlantic. *Deep-Sea Res. II* 58:1819–32
Rhein M, Rintoul SR, Aoki S, Campos E, Chambers D, et al. 2013. Observations: ocean. In *Climate Change 2013: The Physical Science Basis. Contribution of Working Group I to the Fifth Assessment Report of the Intergovernmental Panel on Climate Change*, ed. TF Stocker, D Qin, G-K Plattner, M Tignor, SK Allen, et al., pp. 255–310. Cambridge, UK: Cambridge Univ. Press

Rignot E, Bamber JL, van Den Broeke MR, Davis C, Li Y, et al. 2008. Recent Antarctic ice mass loss from radar interferometry and regional climate modeling. *Nat. Geosci.* 1:106–10

Roemmich D, Church J, Gilson J, Monselesan D, Sutton P, Wijffels S. 2015. Unabated planetary warming and its ocean structure since 2006. *Nat. Clim. Change* 5:240–45

Roemmich D, Gilson J, Davis R, Sutton P, Wijffels S, Riser S. 2007. Decadal spinup of the South Pacific subtropical gyre. *J. Phys. Oceanogr.* 37:162–73

Roemmich D, Wunsch C. 1984. Apparent changes in the climate state of the deep North Atlantic Ocean. *Nature* 307:447–50

Sabine CL, Feely RA, Gruber N, Key RM, Lee K, et al. 2004. The oceanic sink for anthropogenic CO_2. *Science* 305:367–71

Sabine CL, Feely RA, Millero FJ, Dickson AG, Langdon C, et al. 2008. Decadal changes in Pacific carbon. *J. Geophys. Res.* 113:C07021

Sabine CL, Tanhua T. 2010. Estimation of anthropogenic CO_2 inventories in the ocean. *Annu. Rev. Mar. Sci.* 2:175–98

Sarmiento JL, Gruber N, Brzezinski MA, Dunne JP. 2004. High-latitude controls of thermocline nutrients and low latitude biological productivity. *Nature* 427:56–60

Sasano D, Takatani Y, Kosugi N, Nakano T, Midorikawa T, Ishii M. 2015. Multi-decadal trends of oxygen and their controlling factors in the western North Pacific. *Glob. Biogeochem. Cycles.* 29, doi:10.1002/2014GB005065

Sloyan BM. 2005. Spatial variability of mixing in the Southern Ocean. *Geophys. Res. Lett.* 32:L18603

Sloyan BM, Rintoul SR. 2001. The Southern Ocean limb of the global deep overturning circulation. *J. Phys. Oceanogr.* 31:143–73

Sloyan BM, Wijffels SE, Tilbrook B, Katsumata K, Murata A, Macdonald AM. 2013. Deep ocean changes near the western boundary of the South Pacific Ocean. *J. Phys. Oceanogr.* 43:2132–41

Smethie WM, Fine RA. 2001. Rates of North Atlantic Deep Water formation calculated from chlorofluorocarbon inventories. *Deep-Sea Res. I* 48:189–215

Smethie WM, LeBel DA, Fine RA, Rhein M, Kieke D. 2007. Strength and variability of the deep limb of the North Atlantic meridional overturning circulation from chlorofluorocarbon inventories. In *Ocean Circulation: Mechanisms and Impacts—Past and Future Changes of Meridional Overturning*, ed. A Schmittner, J Chiang, S Hemming, pp. 119–30. Geophys. Monogr. 173. Washington, DC: Am. Geophys. Union

Sonnerup RE, Mecking S, Bullister JL. 2013. Transit time distributions and oxygen utilization rates in the Northeast Pacific Ocean from chlorofluorocarbons and sulfur hexafluoride. *Deep-Sea Res. I* 72:61–71

Sonnerup RE, Mecking S, Bullister JL, Warner MJ. 2015. Transit time distributions and oxygen utilization rates from chlorofluorocarbons and sulfur hexafluoride in the Southeast Pacific Ocean. *J. Geophys. Res.* 120(5): 3761–3776. doi: 10.1002/2015JC010781

Sparrow M, Chapman P, Gould J, eds. 2005–2013. *The World Ocean Circulation Experiment (WOCE) Hydrographic Atlas Series*. Southampton, UK: Int. WOCE Proj. Off. http://woceatlas.ucsd.edu

Stanley RHR, Doney SC, Jenkins WJ, Lott DEI. 2012. Apparent oxygen utilization rates calculated from tritium and helium-3 profiles at the Bermuda Atlantic Time-series Study site. *Biogeosciences* 9:1969–83

Stendardo I, Gruber N. 2012. Oxygen trends over five decades in the North Atlantic. *J. Geophys. Res.* 117:C11004

Stramma L, Oschlies A, Schmidtko S. 2012. Mismatch between observed and modeled trends in dissolved upper-ocean oxygen over the last 50 yr. *Biogeosciences* 9:4045–57

Stramma L, Schmidtko S, Levin LA, Johnson GC. 2010. Ocean oxygen minima expansions and their biological impacts. *Deep-Sea Res. I* 57:587–95

Sweeney C, Gloor E, Jacobson AJ, Key RM, McKinley G, et al. 2007. Constraining global air-sea exchange for CO_2 with recent bomb ^{14}C measurements. *Glob. Biogeochem. Cycles* 21:GB2015

Swift JH, Orsi AH. 2012. Sixty-four days of hydrography and storms: RVIB *Nathaniel B. Palmer*'s 2011 S04P Cruise. *Oceanography* 25(3):54–55

Takahashi T, Sutherland SC, Wanninkhof R, Sweeney C, Feely R, et al. 2009. Climatological mean and decadal change in surface ocean pCO_2, and net sea–air CO_2 flux over the global oceans. *Deep-Sea Res. I* 56:2075–76

Takatani Y, Kojima A, Iida Y, Nakano T, Ishii M, et al. 2014. *Ocean acidification in the interior of the western North Pacific subtropical region*. Presented at Int. Ocean Res. Conf., 2nd, Barcelona, Spain, Nov. 17–21

Takatani Y, Sasano D, Nakano T, Midorikawa T, Ishii M. 2012. Decrease of dissolved oxygen after the mid-1980s in the western North Pacific subtropical gyre along the 137°E repeat section. *Glob. Biogeochem. Cycles* 26:GB2013

Talley LD. 2008. Freshwater transport estimates and the global overturning circulation: shallow, deep and throughflow components. *Prog. Oceanogr.* 78:257–303

Talley LD. 2009. Review of ocean temperature, salinity and oxygen changes in the Pacific and subtropical southern hemisphere. *IOP Conf. Ser. Earth Environ. Sci.* 6:032009

Talley LD. 2013. Closure of the global overturning circulation through the Indian, Pacific and Southern Oceans: schematics and transports. *Oceanography* 26(1):80–97, http://dx.doi.org/10.5670/oceanog.2013.07

Tanhua T, Bates NR, Körtzinger A. 2013a. The marine carbon cycle and ocean carbon inventories. In *Ocean Circulation and Climate: A 21st Century Perspective*, ed. J Church, J Gould, S Griffies, G Siedler, pp. 787–815. Int. Geophys. Ser. Vol. 103. Amsterdam: Academic. 2nd ed.

Tanhua T, Waugh DW, Bullister JL. 2013b. Estimating changes in ocean ventilation from early 1990s CFC-12 and late 2000s SF_6 measurements. *Geophys. Res. Lett.* 40:927–32

Tanhua T, Waugh DW, Wallace DWR. 2008. Use of SF_6 to estimate anthropogenic CO_2 in the upper ocean. *J. Geophys. Res.* 113:C04037

Thompson DWJ, Wallace JM, Hegerl GC. 2000. Annular modes in the extra-tropical circulation. Part II: trends. *J. Clim.* 13:1018–36

van Heuven SMAC, Hoppema M, Huhn O, Slagter HA, de Baar HJW. 2011. Direct observation of increasing CO_2 in the Weddell Gyre along the Prime Meridian during 1973–2008. *Deep-Sea Res. II* 58:2613–35
Walker SJ, Weiss RF, Salameh PK. 2000. Reconstructed histories of the annual mean atmospheric mole fractions for the halocarbons CFC-11, CFC-12, CFC-113, and carbon tetrachloride. *J. Geophys. Res.* 105:14285–96
Wanninkhof R, Doney SC, Bullister JL, Levine NM, Warner M, Gruber N. 2010. Detecting anthropogenic CO_2 changes in the interior Atlantic Ocean between 1989 and 2005. *J. Geophys. Res.* 115:C11028
Wanninkhof R, Park G-H, Takahashi T, Feely RA, Bullister JL, Doney SC. 2013a. Changes in deep-water CO_2 concentrations over the last several decades determined from discrete pCO_2 measurements. *Deep-Sea Res. I* 74:48–63
Wanninkhof R, Park G-H, Takahashi T, Sweeney C, Feely R, et al. 2013b. Global ocean carbon uptake: magnitude, variability and trends. *Biogeosciences* 10:1983–2000
Warner MJ, Weiss RF. 1985. Solubilities of chlorofluorocarbons 11 and 12 in water and seawater. *Deep-Sea Res. A* 32:1485–97
Waterhouse A, MacKinnon JA, Nash JD, Alford MH, Kunze E, et al. 2014. Global patterns of diapycnal mixing from measurements of the turbulent dissipation rate. *J. Phys. Oceanogr.* 44:1854–72
Waters JF, Millero FJ, Sabine CL. 2011. Changes in South Pacific anthropogenic carbon. *Glob. Biogeochem. Cycles* 25:GB4011
Waugh DW, Hall TM, Haine TWN. 2003. Relationships among tracer ages. *J. Geophys. Res.* 108:3138
Waugh DW, Primeau F, Devries T, Holzer M. 2013. Recent changes in the ventilation of the Southern Oceans. *Science* 339:568–70
Whalen CB, MacKinnon JA, Talley LD, Waterhouse AF. 2015. Estimating the mean diapycnal mixing using a finescale parameterization. *J. Phys. Oceanogr.* 45:1174–88
Whalen CB, Talley LD, MacKinnon JA. 2012. Spatial and temporal variability of global ocean mixing inferred from Argo profiles. *Geophys. Res. Lett.* 39:L18612
Whitney FA, Bograd SJ, Ono T. 2013. Nutrient enrichment of the subarctic Pacific Ocean pycnocline. *Geophys. Res. Lett.* 40:2200–5
Whitney FA, Freeland HJ, Robert M. 2007. Persistently declining oxygen levels in the interior waters of the eastern subarctic Pacific. *Prog. Oceanogr.* 75:179–99
Wunsch C, Heimbach P. 2013. Two decades of the Atlantic meridional overturning circulation: anatomy, variations, extremes, prediction, and overcoming its limitations. *J. Clim.* 26:7167–86
Yashayaev I. 2007. Hydrographic changes in the Labrador Sea, 1960–2005. *Prog. Oceanogr.* 73:242–76
Yool A, Popova EE, and Anderson TR. 2013a. MEDUSA-2.0: an intermediate complexity biogeochemical model of the marine carbon cycle for climate change and ocean acidification studies. *Geosci. Model Dev*., 6, 1767-1811, doi:10.5194/gmd-6-1767-2013
Yool A, Popova EE, Coward AC, Bernie D, Anderson TR. 2013b. Climate change and ocean acidification impacts of lower trophic levels and the export of organic carbon to the deep ocean. *Biogeosciences* 10:5831–54

Zamora L, Landolfi A, Oschlies A, Hansell D, Dietze H, Dentener F. 2010. Atmospheric deposition of nutrients and excess N formation in the North Atlantic. *Biogeosciences* 7:777–93

Zhang JZ, Mordy CM, Gordon LI, Ross A, Garcia HE. 2000. Temporal trends in deep ocean Redfield ratios. *Science* 289:1839a

Zweng MM, Reagan JR, Antonov JI, Locarnini RA, Mishonov AV, et al. 2013. *World Ocean Atlas 2013, Volume 2: Salinity.* S Levitus, Ed., A Mishonov Technical Ed.; NOAA Atlas NESDIS 74, 39 pp.

RELATED RESOURCES

Feely RA, Fabry VJ, Dickson AG, Gattso J-P, Bijma J, et al. 2010. An international observational network for ocean acidification. In *Proceedings of OceanObs'09: Sustained Ocean Observations and Information for Society, Venice, Italy, 21–25 September 2009*, Vol. 2: *Community White Papers*, ed. J Hall, DE Harrison, D Stammer, chap. 29. ESA Publ. WPP-306. Paris: Eur. Space Agency. http://www.oceanobs09.net/proceedings/cwp/cwp29

GO-SHIP. 2015. *The Global Ocean Ship-Based Hydrographic Investigations Program*. http://www.go-ship.org

Hood M, Fukasawa M, Gruber N, Johnson GC, Körtzinger A, et al. 2010. Ship-based repeat hydrography: a strategy for a sustained global program. In *Proceedings of OceanObs'09: Sustained Ocean Observations and Information for Society*, Vol. 2: *Community White Papers*, ed. J Hall, DE Harrison, D Stammer, chap. 42. ESA Publ. WPP-306. Paris: Eur. Space Agency. http://www.oceanobs09.net/proceedings/cwp/cwp42

Hood EM, Sabine CL, Sloyan BM, eds. 2010. *The GO-SHIP repeat hydrography manual: a collection of expert reports and guidelines*. IOCCP Rep. 14, ICPO Publ. Ser. 134. http://www.go-ship.org/HydroMan.html

Supplemental Appendix 1 to
Changes in Ocean Heat, Ventilation and Overturning: Review of the First Decade of Global Repeat Hydrography (GO-SHIP)
Talley et al. (Annual Reviews of Marine Science)

Organization and Data Policies of Global Ocean Ship-based Hydrographic Investigations Program (GO-SHIP)

The scientific results highlighted in the text of this paper are based principally on measurements collected aboard research ships in every ocean basin. Ship-based hydrography remains the only method for obtaining coincident high-quality, high spatial and vertical resolution measurements of a suite of physical, chemical, and biological parameters over the full water column. These sections also provide important observations of other parameters, including full water-column velocity measurements and underway sampling of ocean surface properties and air-sea fluxes. Moreover, they are increasingly important for deployment and concurrent validation measurements for new sensors on profiling floats. In this supplement, we present information about the ongoing, internationally-coordinated, ship-based measurement program that encompasses these observations.

S1. GO-SHIP: History and program goals

Global hydrographic surveys have been carried out approximately every decade since the 1950s through research programs such as IGY, IIOE, GEOSECS, WOCE / JGOFS, and CLIVAR (acronyms in Supplemental Table 1). In 2009 the Global Ocean Ship-based Hydrographic Program (GO-SHIP, http://www.go-ship.org) was established as part of the Global Climate Observing System (GCOS) as a component of the Global Ocean Observing System (GOOS) to provide international coordination and scientific oversight of the decadal global ocean survey.

GO-SHIP is the systematic and global survey of select hydrographic sections, carried out by an international consortium of ~11 countries and laboratories (Figure S1). These span all of the major ocean basins and the full-depth water column with measurements of the climate accuracy, attainable only with research ships at present and for the foreseeable future.

The GO-SHIP principal scientific objectives are: (1) understanding and documenting the large-scale ocean water property distributions, their changes, and drivers of those changes, and (2) addressing questions of the large physical, biogeochemical and biological changes anticipated for the future ocean. This includes increasing dissolved inorganic carbon, warming, acidification, and increased stratification due to atmospheric CO_2 increases and associated changes in the Earth's radiation balance. The observations will aid understanding of interaction of anthropogenic perturbations with natural cycles of water and sea-ice and with changes in circulation and ventilation processes.

GO-SHIP also provides high-quality reference observations to other components of the Global Ocean Observing System that use autonomous observing platforms (e.g. Argo and SOOP) and supports validation and development of regional and global climate models. The data are freely available in a timely manner to the scientific and general community from a number of data servers, including the CLIVAR and Carbon Hydrographic Data Office (CCHDO; http://cchdo.ucsd.edu/) and the Carbon Dioxide Information Analysis Center (CDIAC; http://cdiac.ornl.gov/oceans/). The GO-SHIP data are used for major assessments of the

role of the ocean in mitigating climate change, research publications, atlases, and outreach materials.

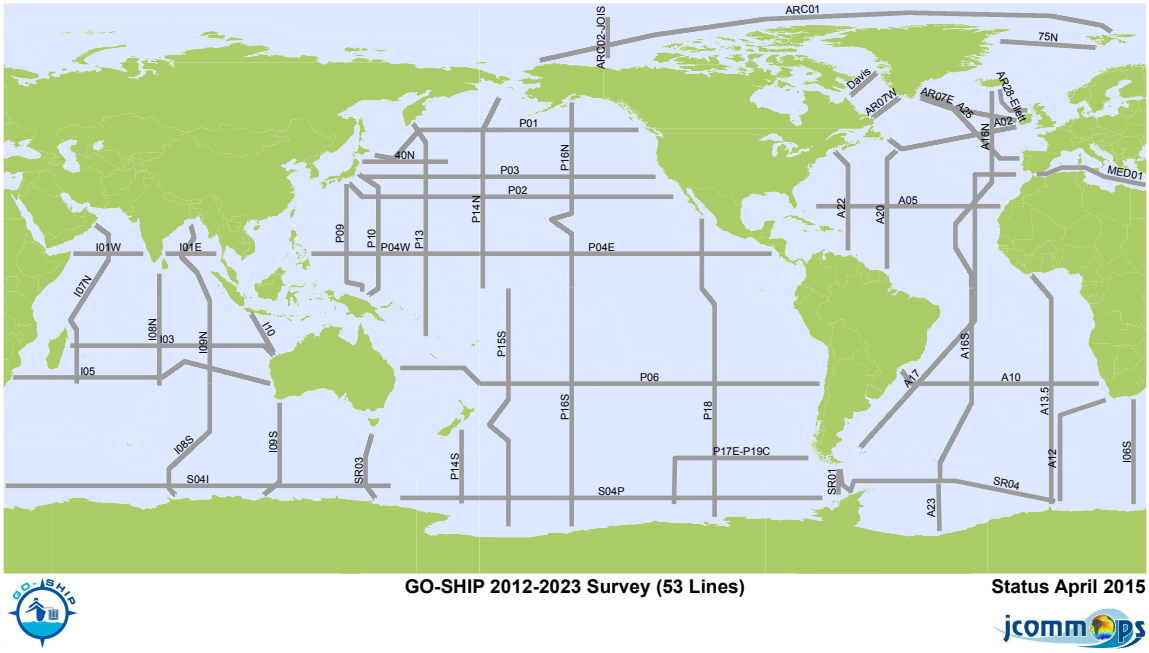

Supplemental Figure 1

The sections of the 2012-2023 campaign of the Global Ocean Ship-based Hydrographic Investigations Program (GO-SHIP) (http://www.go-ship.org).

Supplemental Table 1 Acronyms and websites

Acronym	Full descriptor	Website if applicable
CCHDO	CLIVAR and Carbon Hydrographic Data Office	http://cchdo.ucsd.edu/
CDIAC	Carbon Dioxide Information Analysis Center	http://cdiac.ornl.gov/oceans/
CLIVAR	Climate and Ocean: Variability, Predictability and Change	http://www.clivar.org/
GCOS	Global Climate Observing System	http://www.wmo.int/pages/prog/gcos/
GEOSECS	Geochemical Ocean Sections Program	(historical) https://archive.org/details/geosecsprogramob00geos http://iridl.ldeo.columbia.edu/SOURCES/.GEOSECS/index.html?Set-Language=en
GO-SHIP	Global Ocean Ship-based Hydrographic Program	http://www.go-ship.org
GOOS	Global Ocean Observing System	http://www.ioc-goos.org/
IGY	International Geophysical Year	http://www.nas.edu/history/igy/
IIOE	International Indian Ocean Expedition	(historical)
IOC	Intergovernmental Oceanographic Commission	http://www.ioc-unesco.org/

JCOMMOPS	Joint WMO IOC Commission for Oceanography and Marine Meteorology in situ Observations Programme Support Centre	http://www.jcommops.org/new/
JGOFS	Joint Global Ocean Flux Study	(historical) http://www1.whoi.edu/
SOOP	Ship Of Opportunity Program	http://www.jcommops.org/soopip/
UNESCO	United Nations Educational, Scientific and Cultural Organization	http://en.unesco.org/
WCRP	World Climate Research Programme	http://wcrp-climate.org/
WOCE	World Ocean Circulation Experiment	(historical) https://www.nodc.noaa.gov/woce/

S2. GO-SHIP Scientific Oversight

The initial GO-SHIP Panel was established in 2007 to develop a strategy for a sustained global repeat hydrography program as a contribution to the OceanObs09 Conference (Hood et al. 2010a). As GO-SHIP established itself as an integral component of the GOOS network, the initial panel has evolved to a more formal Executive Group and Further Members committee. Current members of the GO-SHIP committees are

GO-SHIP Committee (2015): Executive Group

Bernadette Sloyan (CSIRO, Australia; co-chair)
Rik Wanninkhof (NOAA, USA; co-chair)
Masao Ishii (MRI-JMA, Japan)
Elaine McDonagh (NOCS, UK)
Takeshi Kawano (JAMSTEC, Japan)
Lynne Talley (SIO, USA)
Toste Tanhua (GEOMAR, Germany)

Martin Kramp (JCOMMOPS) serves as project coordinator

GO-SHIP Committee (2015): Further Members

Leif Anderson (U. Gothenburg, Sweden)
Isabelle Ansorge (UCT, South Africa)
Kumiko Azetsu-Scott (BIO, Canada)
Richard Feely (NOAA, USA)
Masao Fukasawa (JAMSTEC, Japan)
Gregory Johnson (NOAA, USA)
Mauricio Mata (FURG, Brazil)
Herle Mercier (IFREMER, France)
Aida F. Rios (CSIC, Spain)
Mike Williams (NIWA, New Zealand)

The main tasks of the GO-SHIP management committees are to:

- *develop* international agreements for a sustained international repeat ship-based hydrography program, including an internationally-agreed strategy and program plan,
- *advocate* for national contributions to this strategy and participation in the global program,
- *provide* a central forum for communication and coordination, and
- *develop* syntheses of hydrographic data, in partnership with national, regional, and global research programs.

The GO-SHIP observing teams are highly qualified and experienced and the observations meet the highest standards necessary ("climate quality"). The strict GO-SHIP data policy is grounded on the assumption that the data are a shared community resource and should be publicly available as soon as possible. The need for high quality GO-SHIP in situ data for

calibration will grow with the increased use of autonomous ocean observing platforms (e.g. floats, gliders, drifting buoys).

S3. Data types

The GO-SHIP measurement suite is largely adopted from the U.S. GO-SHIP guidelines and endorsed by all international participating nations. They are divided into three levels in order of priority (Supplemental Table 2). These data provide approximately decadal resolution of the changes in inventories and transport of heat, freshwater, carbon, oxygen, nutrients and transient tracers, covering the ocean basins from coast to coast and full depth (top to bottom).

Level 1 core measurements are mandatory on all cruises, and include standard hydrographic and tracer profiling, and velocity profiling. The rationale for classifying a measurement as Level 1 is based on data required to directly quantify change in ocean carbon inventory, estimate anthropogenic CO_2 empirically, characterize large-scale water mass ventilation rates, constrain horizontal heat, freshwater, carbon, nitrogen, and oxygen transports and/or net divergence, and provide an ongoing basis for model evaluation.

Level 2 measurements are highly desirable on a subset of cruises. They may be collected on coarser station spacing and are closely coordinated with the core effort.

Level 3 ancillary measurements are done according to opportunity and space available. They should not significantly interfere with Level 1 or 2 efforts, and may be regional or specific to an individual cruise. They include new technologies and measurement techniques.

The priority of measurements is periodically assessed and parameters are changed to different levels. For example, SF_6 and pH changed from level 2 to level 1 due to improved measurement techniques and increased importance as ventilation and acidification tracers, respectively (e.g. Feely et al. 2010). Measurement standards for all Level 1 and 2 measurements should adhere to or be higher than those set by the GO-SHIP repeat hydrography manual (Hood et al. 2010b), which update standards laid out originally in the WOCE manuals (http://cchdo.ucsd.edu/policy). These measurement standards are routinely reviewed and updated. Certified reference materials are used for all measurements where such standards are available.

Supplemental Table 2 GO-SHIP Measurement and Data Release Schedule[a]

Level 1: (*All data are to be released in final form 6 months after the cruise except where noted*)
Inorganic carbon system parameters: Dissolved inorganic carbon (DIC); Total Alkalinity (TAlk); pH (two of three) (2P); CTD pressure, temperature, conductivity (salinity) (1,2); CTD oxygen (sensor) (2P); Bottle salinity (2); Nutrients by standard auto analyzer (NO_3/NO_2, PO_4, SiO_3) (2); Dissolved oxygen (2P); Chlorofluorocarbons (CFC-11, CFC-12) and SF_6 (2P); Surface underway parameters (T, S, pCO_2) (1); ADCP shipboard (2P); ADCP lowered (2P); Underway navigation and bathymetry (2); Meteorological data (1).
Level 2: (*All data are to be released in final form 6 months after the cruise except where noted*)

Examples include discrete pCO_2 (2); N_2O (2); ^{14}C (3); CCl_4 (2); $\partial\,^{13}C$ of DIC (3); Dissolved organic carbon; dissolved organic nitrogen; $^{3}H/^{3}He$ (4); Fe/trace metals; CTD Transmissometer; Surface underway measurements (nutrients, O_2, Chl, pH, DIC, TAlk, skin temperature).

Level 3: (*All data are to be released in final form within 2 years of analysis*)
Examples include, but are not limited to, microstructure/turbulence; chlorophyll; Primary production; HPLC pigments; Experimental continuous analyzers; $\partial\,^{15}N$; NO_3; ^{32}Si; $\partial\,^{18}O$ of H_2O; NH_4; Low level nutrients; Total organic phosphorus; Upper ocean optical; isotopes of O_2; N_2, Ar, O_2; Methyl halides; DMS.

[a]Notes
(1) Data available daily during the cruise.
(2) Data released to the relevant data management structure within 5 weeks of the cruise; (2P) in preliminary form.
(3) Data released within 6 months of shore-based analysis.
(4) Data released within 15 months of sample collection.

S4. Data policies

The GO-SHIP data policy is stringent and geared toward rapid, open dissemination, with a clear structure for all data to undergo quality control and to be sent to and available from recognized data centers. The policy includes: 1) All Level 1 and 2 observations, cruise reports, and metadata are made public in preliminary form through a specified data center soon after collection ("early release"), with final calibrated data provided six months after the cruise, with the exception of those data requiring on-shore analyses (see Supplemental Table 2). 2) All data collected as part of the program are submitted to a designated data management structure for quality control and dissemination for synthesis.

S5. Future Science and Monitoring Objectives

GO-SHIP builds on previous global-scale hydrography efforts. The program evolves based on the findings of the previous work and emerging science requirements and technological developments. A future development will include addition of further biogeochemistry and biology measurements to enable GO-SHIP to determine trends and variability in marine biogeochemistry and ecosystems. These objectives will be incorporated into the sustained primary objectives of GO-SHIP.

GO-SHIP will continue to provide and expand its capacity to provide a mechanism for testing and validating new autonomous sensors and serve as a reference/calibration dataset for other observing system. As biogeochemical and biological sensors are added to these autonomous platforms, the GO-SHIP data will be invaluable for validating and calibrating these new sensors, and providing high-quality data for algorithm development of carbon system parameters from temperature salinity and oxygen data (Juranek et al. 2011). Microstructure instrument for direct estimates of ocean mixing are being included on select cruises. In addition, the global hydrographic survey will continue to provide a means to access remote ocean areas for the deployment of all autonomous observing platforms.

S6. Summary

The international hydrographic surveys of the 1960s, 1990s (WOCE) and 2000s (CLIVAR Repeat Hydrography and GO-SHIP) were successful in answering many first-

order questions about large-scale ocean circulation and carbon inventories. Their results also raised many new questions concerning ocean variability and trends, circulation, and biogeochemical controls on carbon and tracer inventories, distributions, and long-term secular trends associated with climate change and ocean acidification. These observations showed that the full-depth ocean exhibits significant interannual variability on top of the expected smooth decadal trend as part of patterns of global change, complicating efforts to detect and attribute human influences on the ocean.

GO-SHIP will continue to build the time-series of full-depth repeat ocean measurements capable of resolving decadal and longer time scale changes in the circulation and property storage (including heat, freshwater, oxygen and carbon) of the global oceans.

LITERATURE CITED

Feely RA, Fabry VJ, Dickson AG, Gattso J-P, Bijma J, Riebesell U, Doney S, Turley C, Saino T, Lee K, Anthony K, Kleypas J. 2010. An international observational network for ocean acidification. *Proceedings of OceanObs'09: Sustained Ocean Observations and Information for Society (Vol. 2*). ed. J Hall, DE Harrison, D Stammer, Venice, Italy, ESA Publication WPP-306, doi:10.5270/OceanObs09.cwp.29

Hood M, Fukasawa M, Gruber N, Johnson GC, Körtzinger A, Sabine C, Sloyan B, Stansfield K, Tanhua T. 2010a. Ship-based repeat hydrography: A strategy for a sustained global program. *Proceedings of OceanObs'09: Sustained Ocean Observations and Information for Society (Vol. 2*), 2009: ed. J Hall, DE Harrison, D Stammer, Venice, Italy, ESA Publication WPP-306, doi:10.5270/OceanObs09.cwp.42

Hood EM, Sabine CL, Sloyan BM, Eds. 2010b. *The GO-SHIP Repeat Hydrography Manual: A Collection of Expert Reports and Guidelines*. IOCCP Report Number 14, ICPO Publication Series Number 134. Available online at http://www.go-ship.org/HydroMan.html

Juranek LW, Feely RA, Gilbert D. 2011. Real-time estimation of pH and aragonite saturation state from Argo profiling floats: Prospects for an autonomous carbon observing strategy. *Geophys. Res. Lett.*, 38, L17603, doi:10.1029/2011GL048580

Supplemental Appendix 2
to
Changes in Ocean Heat, Ventilation and Overturning: Review of the First Decade of Global Repeat Hydrography (GO-SHIP)
Talley et al. (submitted Ann. Rev. Mar. Sci.)

Additional figures for Changes in ocean heat, carbon and ventilation (GO-SHIP)

A wide range of topics based on global hydrographic measurements is presented in this review paper; as a result, even with streamlined coverage of the topics, there is inadequate space for illustrations. The authors wish to provide additional figures such that presentations on this material can be relatively complete. Within this supplement we therefore provide additional figures based on those appearing in the Feely et al. (2014) review. "Figure S1" refers to the figure appearing in Supplement 1, which is background for GO-SHIP.

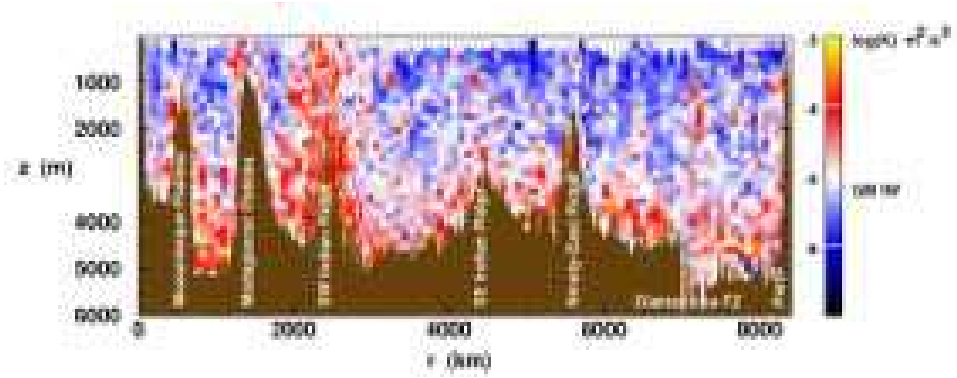

Supplemental Figure 2 for Section 3.3

Diapycnal diffusivity κ along 32°S in the Indian Ocean, estimated from CTD and LADCP profiles (Kunze et al. 2006) using a finescale parameterization, representative of numerous recent studies (e.g., Polzin et al. 2014). The very low values in the thermocline (< 10^{-5} m^2/s^2) are similar to those found in thermocline tracer release experiments (e.g. Ledwell et al. 1998). The increase to values of order 10^{-4} m^2/s^2) in the bottom 1000 m or so of the ocean results from turbulence induced by interaction of internal waves with the bottom. Over especially rough topography and in the presence of strong internal tides, high diffusivities extend almost to the sea surface (e.g. Madagascar Plateau and SW Indian Ridge in this example).

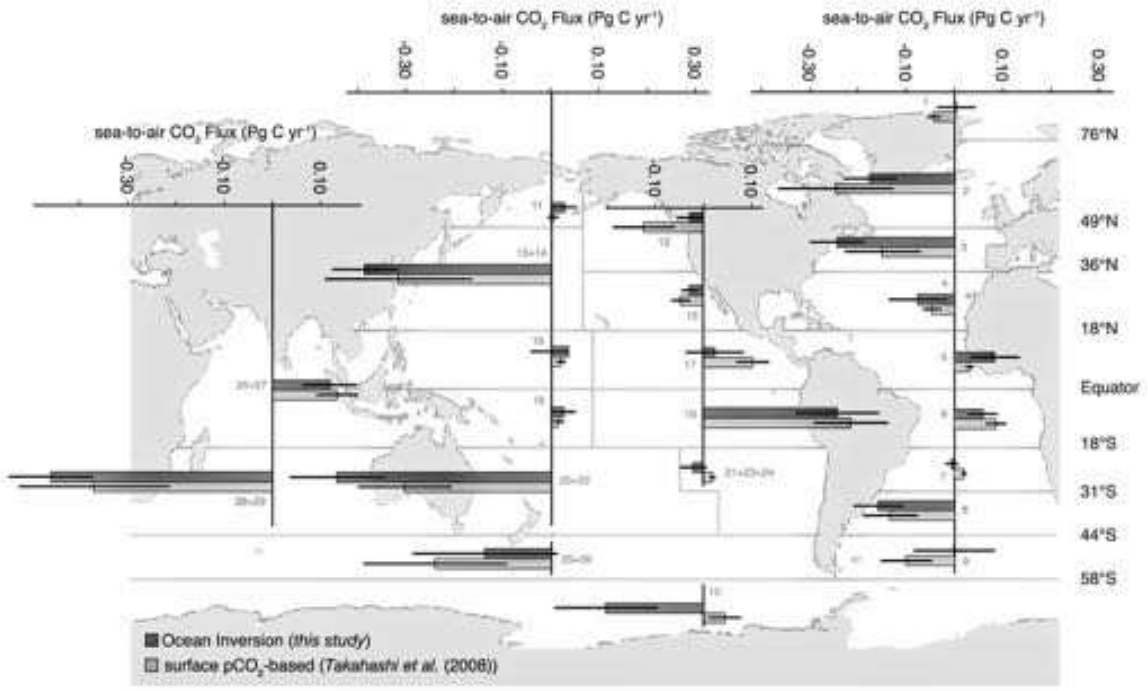

Supplemental Figure 3 for Section 4.1

Comparison of the ocean inversion estimate of sea-to-air CO_2 flux with that based on the CO_2 climatology of Takahashi et al. (2009; from Gruber et al., 2009). The fluxes are for a nominal year of 2000. Positive values indicate net fluxes from sea to air (outgassing), and negative values net fluxes from air to sea (uptake).

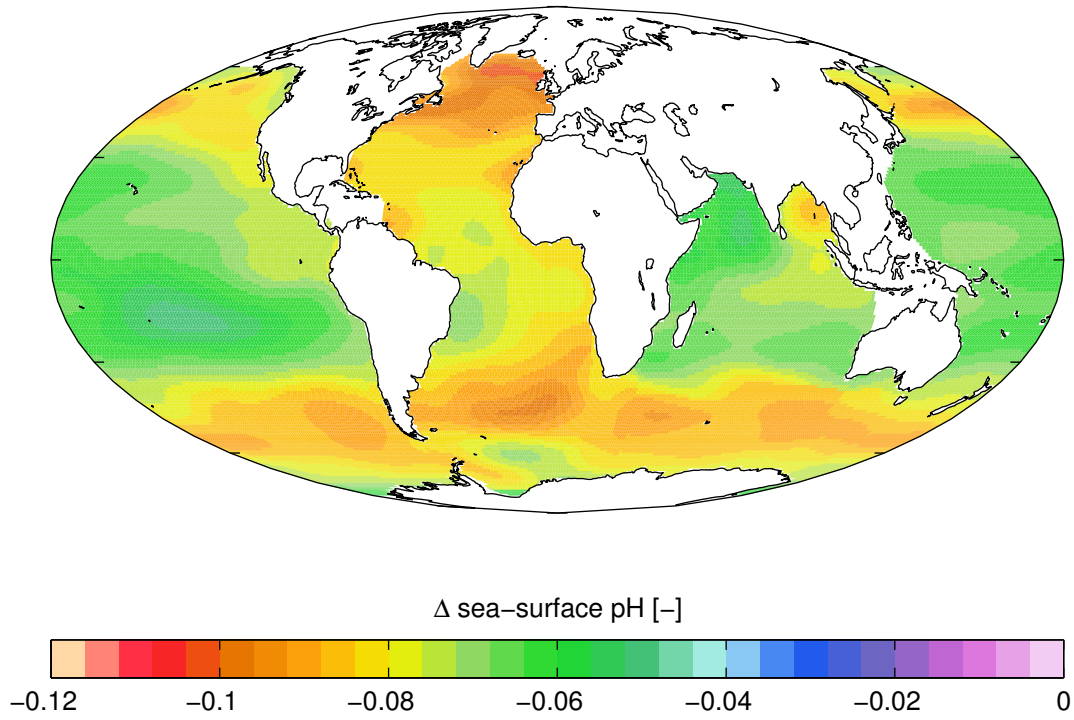

Supplemental Figure 4 for Section 4.1

Estimated surface ocean pH change from the preindustrial to the present, using the GLODAP (Key et al. 2004) and World Ocean Atlas 2005 data products (Antonov et al. 2006, Locarnini et al. 2006), and the csys routine (Zeebe & Wolf-Gladrow 2001), calculated as for the 1990s pH map in Yool et al. (2013).

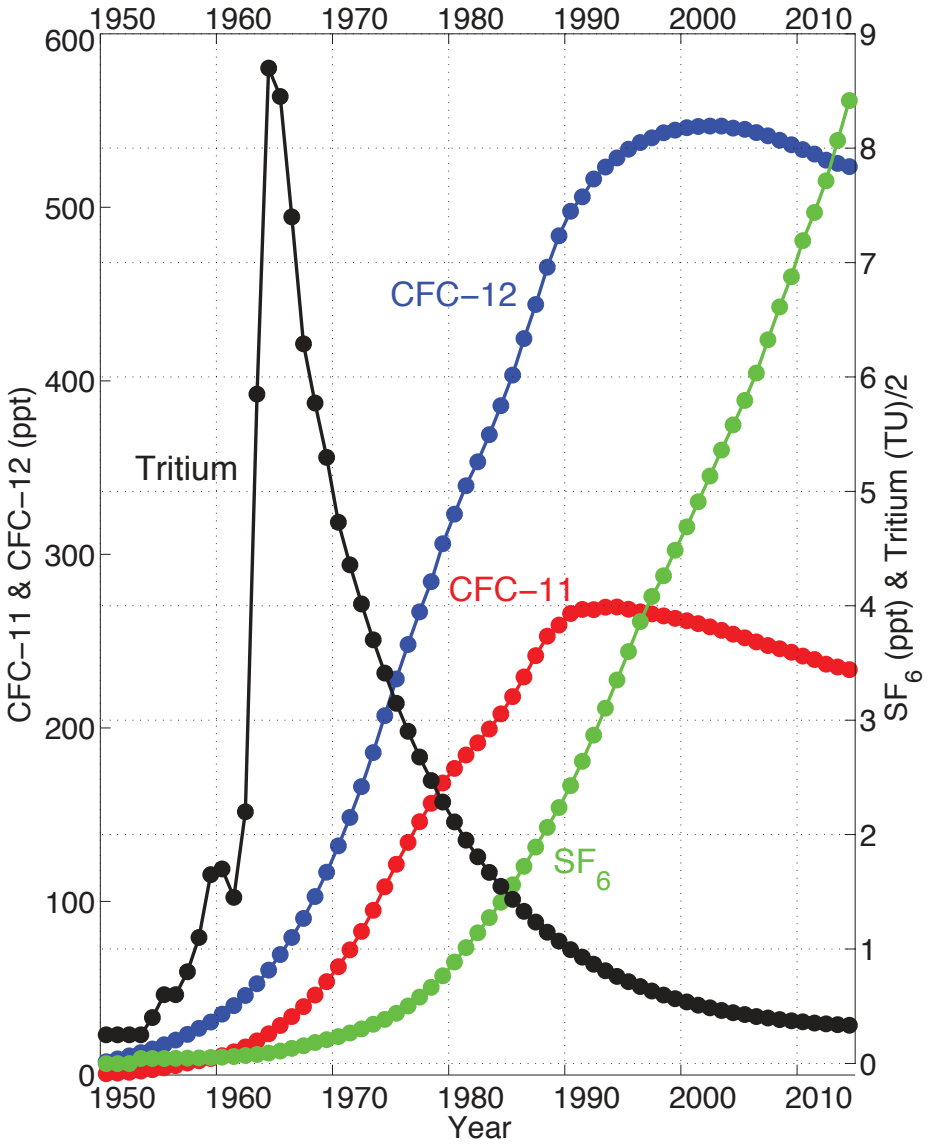

Supplemental Figure 5 for Section 5.1

Time series of atmospheric CFC-11, CFC-12 and SF_6 in the Northern Hemisphere atmosphere (Bullister, 2014) and tritium in North Atlantic ocean surface water at Bermuda (Stanley et al, 2012).

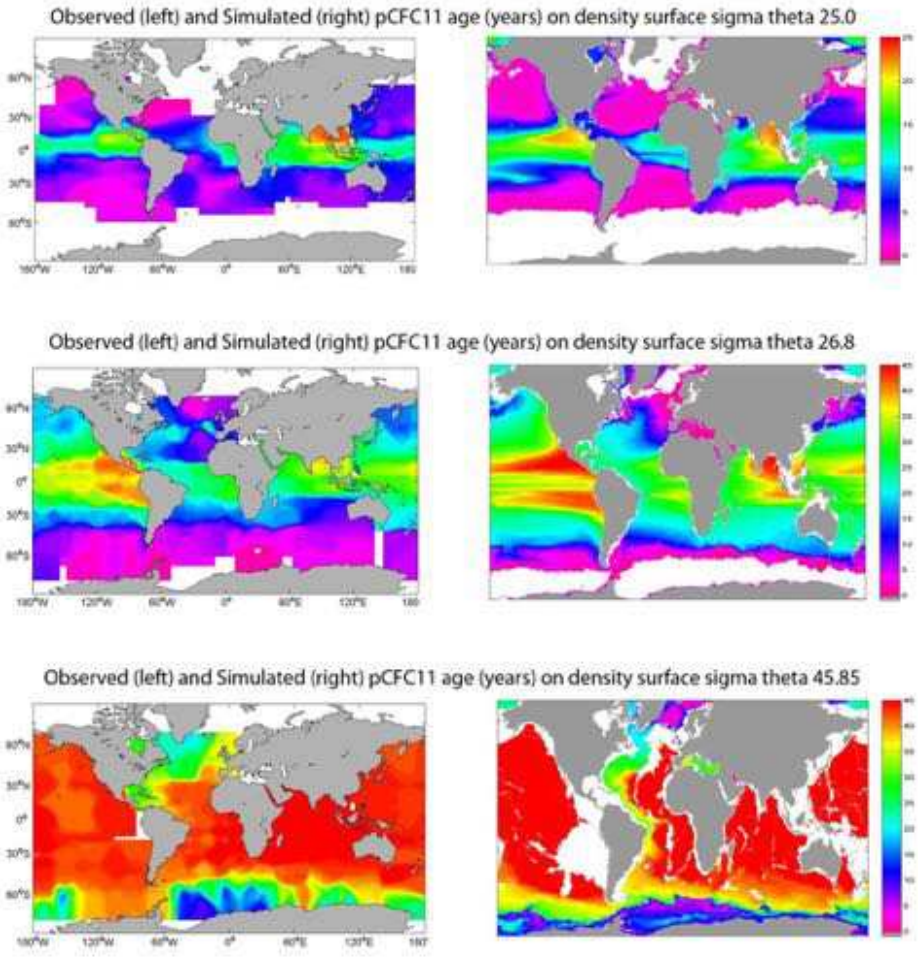

Supplemental Figure 6 for Section 5.1

Global maps of pCFC-11 age in years from WOCE observations (left) and CCSM4 model output for 1994 (right). Color bar on the right shows 0–25 years for 25.0 σ_θ, and 0–45 years for 26.8 σ_θ and 45.85 σ_{4000}. The plots on the right show the native model grid, which is a tripole grid, hence the apparent distortion of the continents in the high latitudes of the Northern Hemisphere. Note that ~45 years is the maximum age given the analytical capability of CFC-11 measurement technique. Thus, ages in regions showing 45 years could be substantially older (after Fine et al. 2014).

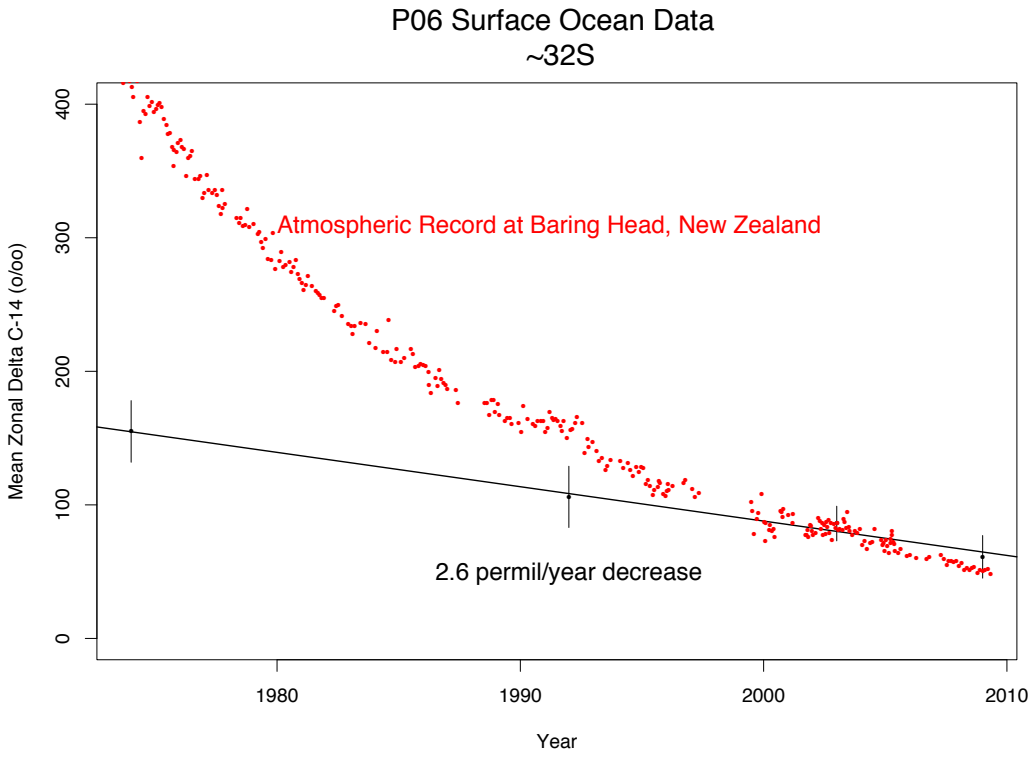

Supplemental Figure 7 for Section 5.2

Time series of atmospheric radiocarbon measurements from New Zealand (red), and averaged ocean surface radiocarbon measurements along 32°S P06 in the South Pacific (black points with error bars) for GEOSECS (1970s), WOCE (1990s), and CLIVAR (GO-SHIP) (2000s) programs. The surface ocean value is decreasing at the average rate of 2.6 parts per thousand per year (black line fit). The huge decrease in atmospheric values is due to the transfer of atmospheric bomb-produced radiocarbon into the surface ocean by gas exchange. For this region, the atmosphere and ocean appear to have reached equilibrium during the first decade of this century. Atmospheric data from Currie et al. (2011) and McNichol et al. (2014).

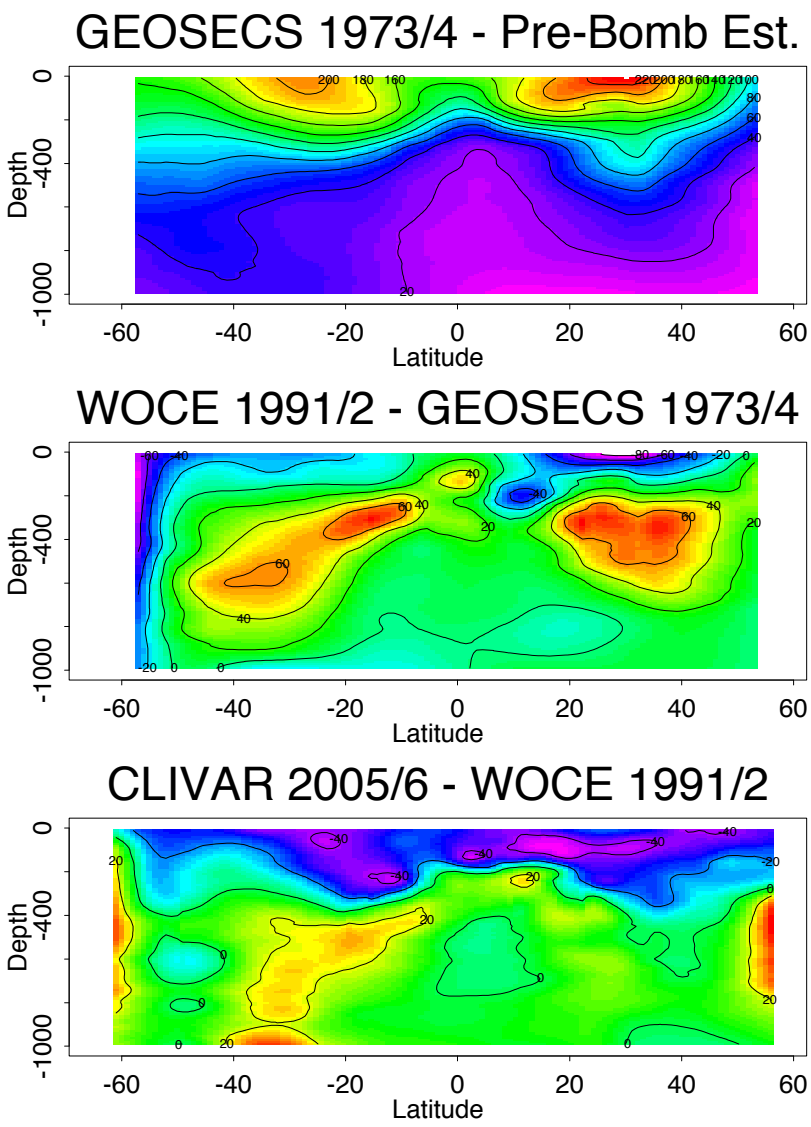

Supplemental Figure 8 for Section 5.2

The estimated change in radiocarbon activity (in parts per thousand) over the indicated time interval along approximately 150°W in the central Pacific Ocean. The red colors depict the transfer of bomb-produced radiocarbon from the atmosphere into the upper ocean and then down into thermocline waters. The subsurface increase occurs primarily in mode and intermediate waters. Colors and contour labels convey the same information in each plot, but the color scales change between panels. In each plot, warm colors represent an increase in radiocarbon while cool colors represent a decrease or no change. Each difference plot was constructed by gridding data along the line of longitude and then subtracting. In the top panel, an estimate of the pre-bomb values (Key et al. 2004) was subtracted from GEOSECS data (using all data east of the dateline). The center and bottom panels were simple differences of measured values from the various programs. During GEOSECS (1970s), the bomb radiocarbon signal was contained in surface or near-surface waters. By the 1990s (WOCE), much of the bomb spike had moved into the upper thermocline. Subsequently, the bomb signal has moved deeper and been more evenly distributed (Graven et al. 2012). Over the second and third interval, the surface concentrations decreased as the radiocarbon moved deeper into the water column.

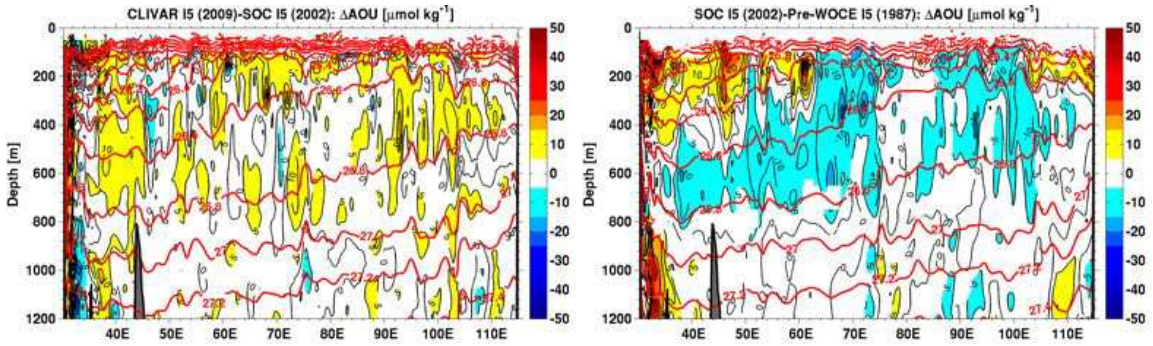

Supplemental Figure 9 for Section 6.1

Changes in apparent oxygen utilization (AOU = O_2 saturation concentration minus measured O_2 concentration) along 32°S in the Indian Ocean: (left) 2009–2002, and (right) 2002–1987 (red = density), using data from the World Ocean Circulation Experiment (WOCE), Southampton Oceanography Centre (SOC) and the most recent GO-SHIP occupation (CLIVAR). The differences were calculated on density surfaces and then projected onto the average depths of the isopycnals (red lines = density contours). The data in the right panel reproduce the 1987 to 2002 increase in O_2 reported by McDonagh et al. (2005) since $\Delta AOU \approx -\Delta O_2$. The data in the left panel indicate a reversal of this signal from 2002 to 2009 (Mecking et al. 2012).

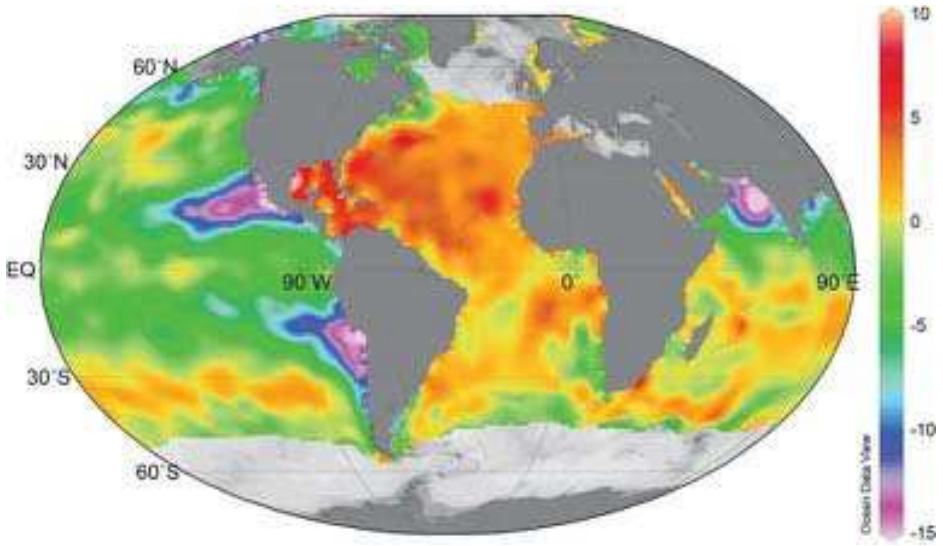

Supplemental Figure 10 for Section 6.2

$N^* = [NO_3^-]-16^*[PO_4^{-3}] + 2.9$ on the 26.5 σ_θ surface using data from the World Ocean Atlas (NODC 2005). Note the large negative N* in the eastern subtropical Pacific Ocean and northern Arabian Seas (denitrification zones) and positive N* in the tropical Atlantic Ocean (from Ryabenko 2013).

LITERATURE CITED

Antonov JI, Locarnini RA, Boyer TP, Mishonov AV, and Garcia HE. 2006. *World Ocean Atlas 2005, Volume 2: Salinity*. S Levitus, Ed. NOAA Atlas NESDIS 62, U.S. Government Printing Office, Washington, D.C., 182 pp

Bullister JL 2014. Atmospheric CFC-11, CFC-12, CFC-113, CCl4, and SF_6 histories (1910–2014). http://cdiac.ornl.gov/oceans/new_atmCFC.html

Currie KI, Gordon B, Nichol S, Gomez A, Sparks R, Lassey KR, and Riedel K. 2011. Tropospheric $^{14}CO_2$ at Wellington, New Zealand: The world's longest record. *Biogeochemistry*, 104, 5–22, doi:10.1007/s10533-009-9352-6

Feely RA, Talley LD, Bullister JL, Carlson CA, Doney SC, et al. 2014. The US Repeat Hydrography CO_2/Tracer Program (GO-SHIP): Accomplishments from the first decadal survey. *US CLIVAR and OCB Report*, 2014-5, US CLIVAR Project Office, 47 pp.

Fine, RA, Peacock S, Maltrud ME, and Bryan FO. 2014. A new look at ocean ventilation timescales. Abstract, *2014 Ocean Sciences Meeting*, Honolulu, Hawaii

Graven HD, Gruber N, Key K, Khatiwala S, Giraud X. 2012. Changing controls on oceanic radiocarbon: New insights on shallow-to-deep ocean exchange and anthropogenic CO_2 uptake. *J. Geophys. Res.*, 117, C10005, doi:10.1029/2012JC008074

Gruber, N, Gloor M, Mikaloff Fletcher SE, Doney SC, Dutkiewicz S, et al. 2009. Oceanic sources, sinks, and transport of atmospheric CO_2. *Global Biogeochem. Cycles*, 23, GB1005, doi: 10.1029/2008GB003349

Key, RM, Kozyr A, Sabine CL, Lee K, Wanninkhof R, et al. 2004. A global ocean carbon climatology: Results from Global Data Analysis Project (GLODAP). *Global Biogeochem. Cycles*, 19, GB4031, doi:10.1029/2004GB002247

Kunze E,Firing E, Hummon JM, Chereskin TK, Thurnherr, AM. 2006. Global abyssal mixing from lowered ADCP shear and CTD strain profiles. *J. Phys. Oceanogr.* 36: 1553–1576, doi:10.1175/ JPO2926.1

Ledwell JR, Watson AJ, Law CS. 1998. Mixing of a tracer in the pycnocline. *J. Geophys Res.* 103, 21499-21529

Locarnini RA, Mishonov AV, Antonov JI, Boyer TP, and Garcia HE. 2006. *World Ocean Atlas 2005, Volume 1: Temperature*. S Levitus, Ed. NOAA Atlas NESDIS 61, U.S. Government Printing Office, Washington, D.C., 182 pp.

McNichol A, Key RM, Jenkins W, Elder K, von Reden K, Gagnon A, Burton J. 2014. The WOCE/ CLIVAR radiocarbon programs—Decadal changes in $\Delta^{14}C$ in the world's oceans. Abstract, *2014 Ocean Sciences Meeting*, Honolulu, Hawaii

Mecking S, Johnson GC, Bullister JL, Macdonald AM. 2012. Decadal changes in oxygen and temperature-salinity relations along 32°S in the Indian Ocean through 2009. Abstract *2012 Ocean Sciences Meeting*. Salt Lake City, Utah

Polzin, KL, Naveira Garabato AC, Huussen TN, Sloyan BM, Waterman S. 2014. Finescale parameterizations of turbulent dissipation. *J. Geophys. Res. Oceans*, 119, doi:10.1002/2013JC008979

Ryabenko E. 2013. Stable isotope methods for the study of the nitrogen cycle. *Topics in Oceanogr.*, E. Zambianchi Ed., InTech, 1-40, doi:10.5772/56105

Stanley RHR, Doney SC, Jenkins WJ, Lott DEI. 2012. Apparent oxygen utilization rates calculated from tritium and helium-3 profiles at the Bermuda Atlantic Time-series Study site. *Biogeosciences*, 9, 1969-1983

Takahashi T, Sutherland SC, Wanninkhof R, Sweeney C, Feely RA, et al. 2009. Climatological mean and decadal change in surface ocean pCO_2, and net sea- air CO_2 flux over the global oceans. *Deep-Sea Res. I*, 56, 2075–2076, doi:10.1016/j.dsr2.2008.12.009

Yool A, Popova EE, and Anderson TR. 2013. MEDUSA-2.0: an intermediate complexity biogeochemical model of the marine carbon cycle for climate change and ocean acidification studies. *Geosci. Model Dev*., 6, 1767-1811, doi:10.5194/gmd-6-1767-2013

Zeebe RE and Wolf-Gladrow DA. 2001. *CO_2 in Seawater: Equilibrium, Kinetics, Isotopes*. Elsevier Oceanography Series, 65, pp. 346, Amsterdam.